Latin American Journal of Aquatic Research, 52(3): 416-442, 2024
DOI: 10.3856/vol52-issue3-fulltext-3124

Research Article

Response of the phytoplankton size fractions along environmental gradients from an oxygen minimum zone in the central Mexican Pacific

David U. Hernández-Becerril[1], Francisco Varona-Cordero[1]
Francisco J. Gutiérrez-Mendieta[2], Erick J. Ponce-Manjarrez[3]
Martín Merino-Ibarra[1], Sofía A. Barón-Campis[4] & Alexis U. Vargas-Reyes[2]
[1]Instituto de Ciencias del Mar y Limnología, Universidad Nacional Autónoma de México
Ciudad de México, México
[2]Departamento de Hidrobiología, Universidad Autónoma Metropolitana (UAM-I)
Unidad Iztapalapa, Iztapalapa, Ciudad de México, México
[3]Departamento de Investigaciones Científicas y Tecnológicas (DICTUS)
Universidad de Sonora, Hermosillo, México
[4]Instituto Mexicano de Investigación en Pesca y Aquacultura Sustentables
Secretaría de Agricultura y Desarrollo Rural (SADER), Ciudad de México, México
Corresponding author: David U. Hernández-Becerril (dhernand@cmarl.unam.mx)

ABSTRACT. The marine phytoplankton community responds to latitudinal, longitudinal (coast to ocean), and vertical environmental gradients, an important subject in Oxygen minimum zones (OMZ). The phytoplankton structure and the effect of environmental gradients along the central Mexican Pacific, an area within an OMZ, were studied, especially the importance of size fractions and taxonomic groups. A combination of various methods and protocols, such as microscopic analysis, flow cytometer, and pigment analysis, were followed in this study. Oceanographic conditions included thermal gradients along the study area and unreported evidence of a weak upwelling in the southern zone (Acapulco). Vertical distribution of chlorophyll *a* showed subsurface maxima (SCM, 15-45 m depth) in all stations, and deeper chlorophyll-*a* maxima (DCM, 85-95 m depth) in more oceanic stations. Chain-forming diatoms dominated in the northern zone stations. *Prochlorococcus*, *Synechococcus*, and picoeukaryotes abundances ranged between 0.01 to 21.7 cells×10^4 mL^{-1}, although most samples showed the highest contribution to biomass (47.95 µg C L^{-1}) by picoeukaryotes. Expected tendencies of *Prochlorococcus* distribution were observed: highest densities coincided with the DCM and divinyl chlorophyll-*a* distribution at oceanic stations. Fucoxanthin had the highest concentrations, whereas fucoxanthin and zeaxanthin concentrations were higher at SCM depths. We documented the co-dominance of the pico- and microplankton: picoplankton was important at the DCM, related to oligotrophic and more stratified water column, whereas microplankton prevailed in coastal stations, with mixed water column, high nutrient concentrations, and diatoms as the dominant group. Picoeukaryotes abundances were related to the concentration of prasinoxanthin, which suggests an important mamiellophyte component not previously revealed.

Keywords: *Prochlorococcus*; *Synechococcus*; Mamiellophytes; microphytoplankton; photosynthetic pigments; picophytoplankton; central Mexican Pacific

Associate Editor: José Luis Iriarte

INTRODUCTION

Microbial communities are very important to understanding many ecological processes in Oxygen minimum zones (OMZ), particularly phytoplankton with its taxonomic and functional groups and the different size fractions that play a key role in productive mechanisms (Ulloa et al. 2012, Wright et al. 2012, Sunagawa et al. 2015). The central Mexican Pacific is a large area of tropical affinity with the particularity of being strongly affected by a conspicuous OMZ. Recent oceanographic studies have revealed high inter- and intra-annual variability and the presence of spring upwelling in the Cabo Corrientes area (Gallegos et al. 2006, López-Sandoval et al. 2009).

Previously published information on the phytoplankton ecology in this area shows aspects such as primary productivity measurements (López-Sandoval et al. 2009, Becerra-Reynoso 2017) and structure of the picoprokaryote fraction (Goericke et al. 2000, Santana-Vega et al. 2018, Pajares et al. 2020). Also, different taxonomic groups have been studied in certain details in this area, including diatoms (Hernández-Becerril 1996, 1998, Hernández-Becerril et al. 2010, 2013), dinoflagellates (Hernández-Becerril & Bravo-Sierra 2004, Hernández-Becerril et al. 2008, Esqueda-Lara & Hernández-Becerril 2010, Escobar-Morales & Hernández-Becerril 2015), silicoflagellates (Hernández-Becerril & Bravo-Sierra 2001), raphidophytes (Band-Schmidt et al. 2004), and cocolithophorids (Hernández-Becerril et al. 2016). Additionally, recurrent red tides and harmful algal blooms have been studied in some points along the coasts of the area (Ortiz-Lira & Jiménez-Quiroz 2006, Hernández-Becerril et al. 2007), and it is now possible to identify some interesting microplanktonic species potentially blooming and producing red tides (Hernández-Becerril et al. 2007, 2012a).

The relative importance of the picophytoplankton community, especially the prokaryote fraction (*Prochlorococcus* and *Synechococcus* populations), and particularly regarding the vertical distribution of chlorophyll-*a* (Chl-*a*), to which this fraction contributes considerably to the biomass of the deep Chl-*a* maxima (DCM), has also been mentioned in the study area (Cepeda-Morales et al. 2009, Márquez-Artavia et al. 2019). *Prochlorococcus* and *Synechococcus* abundances have been compared with those found in other tropical areas, with similar results (Santana-Vega et al. 2018). Previously, Goericke et al. (2000) had detected considerably high densities of the picocyanobacterial *Prochlorococcus*, deeper than the oxygen minimum layers, in the south portion of the central Mexican Pacific, which was confirmed later (Santana-Vega et al. 2018). Regarding picoeukaryotes, the eukaryotic fraction between 30 and 1.6 μm size has been reported (Duret et al. 2015). In contrast, this fraction was also recently analyzed, showing its importance in subsurface layers at coastal stations (Pajares et al. 2020). However, this fraction's detailed composition (e.g. taxonomic groups and their proportions) is still missing.

The combined use of different analytical methods for studying marine phytoplankton, such as picophytoplankton analysis (by flow cytometry) and photosynthetic pigment determination (by HPLC), has added information to the traditional microscopic observations (species identifications and cell counts) and cell density calculations, and offer a complete picture of the importance of taxonomic groups and size fractions (Veldhuis & Kraay 1990, Suzuki et al. 2005, Tamm et al. 2018).

We postulate that phytoplankton, and especially the picoplankton fraction, should respond to the environmental latitudinal, coast-to-ocean, and vertical gradients present in the area, changing in composition and abundance and that it should be a differential vertical distribution generating layers dominated by different phytoplankton groups and fractions according to their physiological preferences, for example, the subsurface chlorophyll maxima (SCM) with higher abundances of diatoms and other micro- and nanoplankton groups, and DCM with higher abundances of picoplankton, particularly *Prochlorococcus*; these gradients are driven by temperature in the latitudinal and the coast-to-ocean axes, and by dissolved oxygen, nutrients and light availability in the vertical axis. We also hypothesize that the picoeukaryote fraction may be well-represented by mamiellophytes. Combining analytical methods (e.g. flow cytometry, photosynthetic pigments, molecular tools) reveals this important contribution, basically considering recent studies showing the relevance of picoplanktonic mamiellophytes, especially in coastal waters (Not et al. 2004, Worden 2006, Worden & Not 2008, Hernández-Becerril et al. 2012b, Yung et al. 2022), and the preliminary metabarcoding results of samples collected from the study area indicating the presence of various species of that group (Hernández-Becerril et al. *in press*).

In this paper, we investigated the basic structure of phytoplankton, considering its composition, abundance, distribution, and signature pigments. During an oceanographic cruise in the central Mexican Pacific, we

focused on the picophytoplankton fraction (both the prokaryote and eukaryote components) and the effect of environmental gradients in an area influenced by an OMZ.

MATERIALS AND METHODS

Study area

This study was conducted in an area of the central tropical Mexican Pacific, located between 16°19' and 20°38'N, and 99°50' and 106°15'W (Fig. 1). This area sustains a great diversity of organisms and important pelagic fisheries, with different mechanisms of natural fertilization such as mesoscale phenomena (plumes and eddies) and upwellings, and shallow thermoclines reducing stratification and keeping relatively high phytoplankton biomass values (López-Sandoval et al. 2009). Another interesting point is that this area is located within an OMZ (Paulmier & Ruiz-Pino 2009, Ulloa et al. 2012, Maske et al. 2019), and some hydrographic features (for instance, thermo- and nutriclines) do affect the vertical distribution of biological properties such as Chl-*a*. Data and samples were measured and collected during the oceanographic cruise "MareaR V," carried out from April 3 to 12, 2013, on board the R/V "El Puma," considering five zones: Cabo Corrientes (CC), Bahías Manzanillo-Santiago (BMS), Maruata (MAR), Lázaro Cárdenas (LC), and Acapulco (ACA) (Figs. 1-2).

Hydrographic data and water sampling

Fifty-nine fixed stations were considered during the cruise (Fig. 1) to obtain hydrographic data (temperature, salinity, dissolved oxygen) in vertical profiles, using a CTD (Seabird SBE 911 PLUS) fitted with an additional sensor for fluorescence (WET Labs ECOAFL/FL), and water samples. Transects perpendicular to the coastline of three to five stations were set for each of the five zones (Fig. 1). For this study, only stations with complete picophytoplankton and phytoplankton pigments data, forming a transect of at least three stations were considered and illustrated. Water samples were collected at five depths (usually 5, 20, 30, 40, and 70 or 100 m), according to the *in situ* fluorescence (Chl-*a*) maximum layers or peaks: A) for phytoplankton microscopic analysis, 250 mL were kept in dark bottles and fixed with Lugol's solution, B) for picophytoplankton analysis, 4.5 mL were placed in cryovials and fixed with 1% glutaraldehyde, C) for phytoplankton pigments, 1 L was filtered with a vacuum pump through GF/F (47 mm diameter) filters; all samples for picophytoplankton and pigments were stored in liquid nitrogen and a -20°C freezer, and D) for nutrient analysis, 20 mL were held in polypropylene containers, after filtration through 0.45 and 0.22 μm (MilliporeTM type HA) nitrocellulose membranes, and were kept frozen (-4°C). Table S1 summarizes all samples obtained and analyzed.

Laboratory analysis

Nutrients

The samples were thawed for analysis in a Skalar San Plus segmented-flow auto-analyzer using the standard methods adapted by Grasshoff et al. (1983) and the circuits suggested by Kirkwood (1994). The precision of the analyses with this system was: nitrate 0.1 μM, nitrite 0.02 μM, ammonium 0.1 μM, soluble reactive phosphorous (SRP) 0.04 μM, and SRSi 0.1 μM. Each sample was analyzed in duplicate. If the two determinations differed by more than twice the accuracy of the analysis, a third determination was made.

Microscopic analysis

Only samples obtained from the transect in CC were studied. Bottle samples were collected at three stations and three depths, E5- 20 (SCM), 40, 83 m, E7- 0, 31 (SCM), 50 m, and E9- 5, 23 (SCM), 40 m, and were fixed with Lugol's solution. They were analyzed following the inverted microscope technique (Utermöhl), using 25 or 50 mL chambers, and settled for 24 h. Identification and counting were made in cross-transects, and phytoplankton density was calculated using the formula recommended by Edler & Elbrächter (2010).

Flow cytometry

Flow cytometry analyses were conducted to recognize and quantify picophytoplankton populations, following the protocol of Marie et al. (1999). Water samples were thawed at room temperature and injected into a FACSCalibur (Becton Dickinson) flow cytometer. The following parameters were considered: forward light scatter (FSC, E01), side light scatter (SSC, 450), and three fluorescence (FL1, 650 green, FL2, 650 orange, and FL3, 650 red). Additionally, 0.95 and 3.0 μm fluorescent microspheres (Becton Dickinson) were used for calibration. Picophytoplankton populations were identified and quantified by analyzing all cytograms with the program Cyflogic 1.2.1.

Factors of 56, 112, and 1010 fg C cell^{-1} were chosen from the literature to calculate picophytoplankton carbon biomass as the most representative and conservative values for *Prochlorococcus*, *Synecho-*

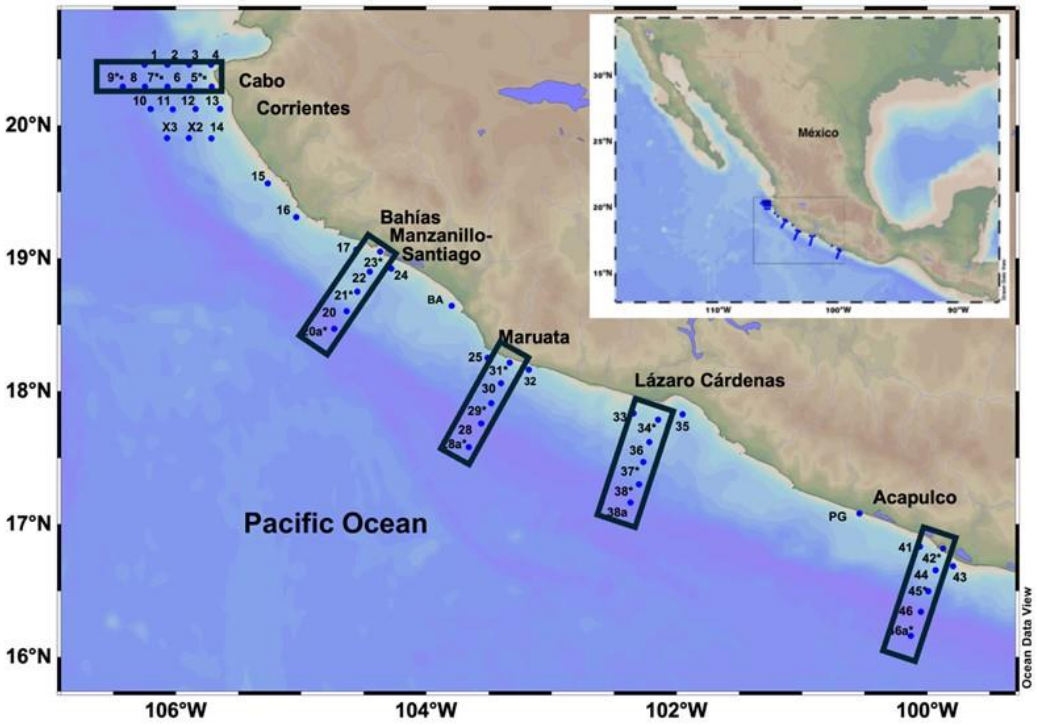

Figure 1. Map showing the study area in the Mexican Pacific, the five different transects, and sampling stations.

coccus, and picoeukaryotes, respectively (Lee & Fuhrman 1987, DuRand et al. 2001, Linacre et al. 2010).

Phytoplankton pigments

For pigments analysis, the HPLC method proposed by Vidussi et al. (1996) was followed, using equipment Hewlett Packard® series 1100, equipped with DAD, FLD, and a software OpenLAB Version A.01.02 with Chem Station Rev 0.01.02 (14). A column ZORBAX Eclipse XD B-C8 of 5 µm and 4.6×150 mm was used. Pigment identification followed the criteria proposed by Wright & Mantoura (1997), where retention times and absorption spectra were compared with original standards. Twelve signature pigments were measured, including Chl-*a*, fucoxanthin (usually used to recognize diatom abundances), peridinin (signature pigment for dinoflagellates), 19' hexanoyloxyfucoxanthin (19' HF) and 19' butanoyloxyfucoxanthin (19' BF) (both signature pigments for haptophytes), zeaxanthin (employed to identify Cyanobacteria, especially the picoplanktonic *Synechococcus*), and divinyl Chl-*a* (pigment characteristic of the picocyanobacteria *Prochlorococcus*). Other pigments measured, alloxanthin, prasinoxanthin, and β-carotene, were detected occasionally or in very low concentrations. Standards of all pigments analyzed were obtained from DHI Lab Products (Hoersholm, Denmark).

Diagnostic pigment indices (DP) and proportions of phytoplankton by size class (pico, nano and microphytoplankton) were derived using the equations described by Barlow et al. (2008) using eight diagnostic pigments: fucoxanthin, peridinin, 19' HF, 19' BF, alloxanthin, total chlorophyll-*b*, (TChl-*b*), zeaxanthin and divinyl Chl-*a*. The pigment indices were calculated as follows: photoprotective carotenoids (PPC) Σ = diadinoxanthin + alloxanthin + diatoxanthin + zeaxanthin + β-carotene) to total pigments (PPC/TP) and photosynthetic carotenoids (PSC) Σ = fucoxanthin + peridinin + 19' hexanoyloxyfucoxanthin + 19' butanoyloxyfucoxan-thin + violaxanthin + Chl-*b*) to total pigments (PSC/TP). This approach has proven valuable in providing the dominant trends of the phytoplankton community and size structure at the regional and seasonal scales (Uitz et al. 2006, Ras et al. 2008).

Winds data

Zonal and meridional (u, v) data of the winds from the study area (data of 1, 5, 8, 10, and 13 April 2013) were obtained from the EROS5 web platform. The trigonometric equation arctg(u/v) ×100 was used to calculate the wind direction (González-Ferreiro & Bosque-Sendra 2008). Surface temperatures were obtained from the Google Earth Engine web platform,

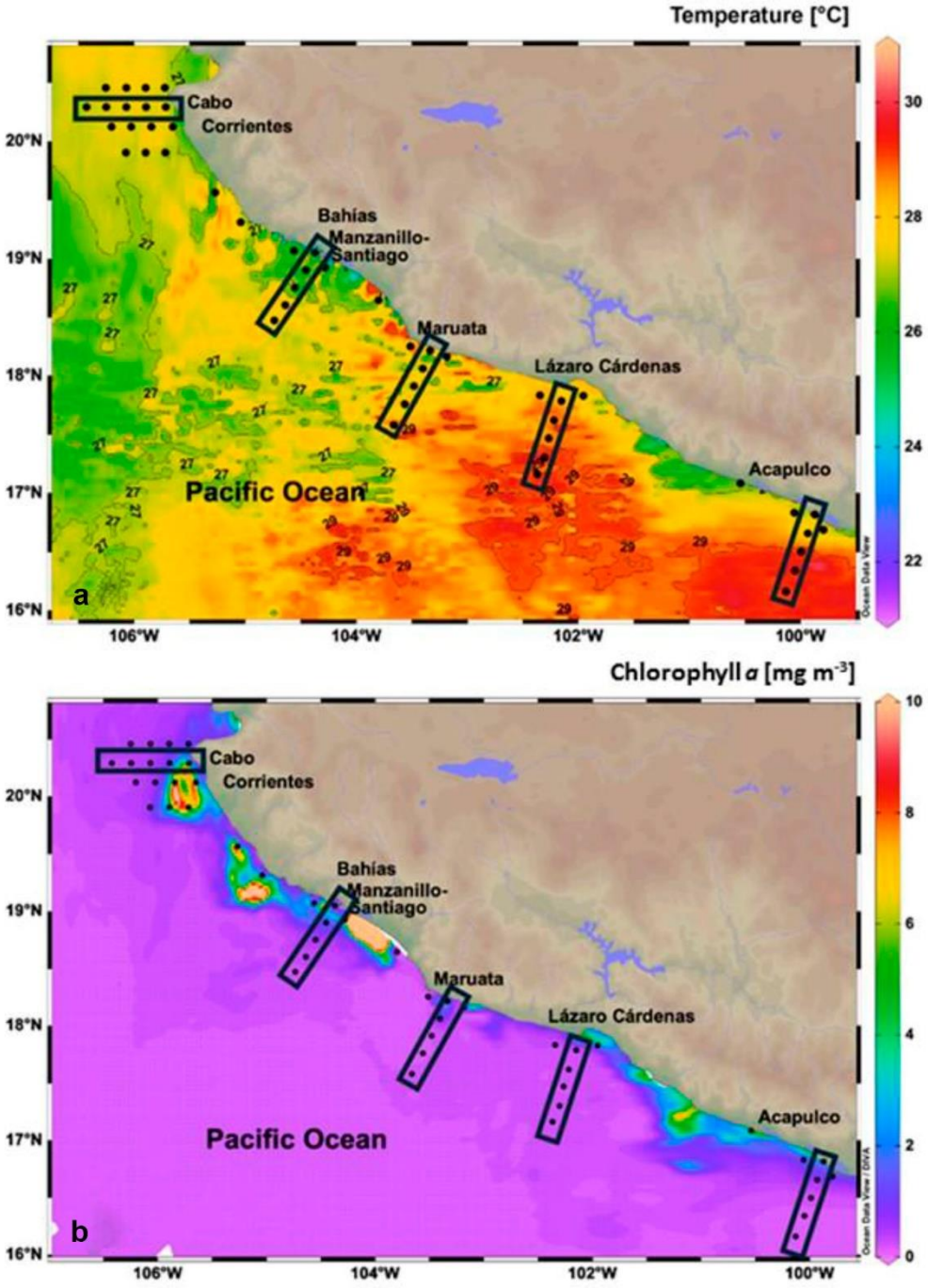

Figure 2. Spatial patterns of remote sensed. a) Sea surface temperature (SST) and b) chlorophyll-*a* of the study area for April 2013. Images were based on (SST): [https://coastwatch.pfeg.noaa.gov/erddap/griddap/index.html?page=1&itemsPerPage=1000], and (chlorophyll-*a*): [https://coastwatch.pfeg.noaa.gov/erddap/griddap/erdMH1chla8day.graph?chlorophyll%5B(2011-0413T00:00:00Z)%5D%5B(27.02083):(24.02083)%5D%5B(-98.02083):(-6.52083)%5D&.draw=surface&.vars=longitude%7Clatitude%7Cchlorophyll&.colorBar=%7C%7C%7C%7C%7C&.bgColor=0xffccccff].

with a spatial resolution of 4 km and a temporal resolution of three days. The open code software QGIS was used to process the satellite data and map design.

Statistical analysis

Multivariate analyses were performed to detect spatial differences in the abundances of the picophytoplankton found and evaluate the contribution of each taxon or

size-fraction to the spatial variability. Principal components analysis (PCA) was performed to explore the most relevant environmental variables responsible for any pattern in the abundance of picophytoplankton, and the PCA was based on the Euclidean distance similarity matrix of the log-transformed variables after the use of Draftsman plots to eliminate highly correlated redundant variables from the analysis (Clarke & Gorley 2006). Abiotic data were used as quantitative variables, and biotic data (picophytoplankton biomass and pigment index) were used as qualitative supplementary variables. PCA was performed with XLSTAT 2018.5 (Base version, Addinsoft).

RESULTS

Hydrographic features, nutrients, and chlorophyll-*a*

A thermal latitudinal gradient and a heterogeneous surface distribution of Chl-*a* were observed in the study area (Figs. 2a-b). In Cabo Corrientes (CC), the Sea surface temperatures (SST) were lower (less than 27°C) in stations located north of the study area. They were increasing (up to 29°C) toward the south stations in Acapulco (ACA) (Fig. 2a). Additionally, lower SST was detected at some coastal zones (Figs. 2a, 3a-d), suggesting upwelling events. The surface distribution of Chl-*a* showed a general pattern of higher concentrations in coastal zones, especially in CC, Bahías Manzanillo-Santiago (BMS), Lázaro Cárdenas (LC), and north of ACA (intermediate smaller zones) (Fig. 2b), in coincidence with the SST (Fig. 2a). This information was compared with our data and we consider they are consistent.

Wind maps (Figs. 3a-d) showed temporal differences of SST, with a strong coincidence with the previous temperature map (Fig. 2a), and the persistence, up to four different days (1, 5, 8 and 10 April 2013) of the direction of the wind, toward south-east, parallel to the cost (Figs. 3a-d), associated to the changes of the SST, particularly lower SST at the same coastal zones as described above (CC, BMS, LC, north of ACA, and intermediate smaller zones) (Figs. 3a-d), adding more evidence for the upwelling occurrence.

All stations (including coastal and oceanic ones) showed a general pattern with defined thermoclines and oxyclines (Figs. 4-7). The depth of the mixed layers was variable: the isotherm of 24°C varied from 24 to 35 m depth in stations of CC, BMS, and Maruata (MAR), and from 12 to 42 m depth in stations in LC and ACA (Figs. 4-7), evidence of relatively cooler water elevation at the coastal stations (St 34, 42) in LC and ACA, respectively. However, only at St 42 was a weak stratification detected, so an unexpected upwelling event was suggested (Figs. 4i, 7e). Dissolved oxygen values were low (2 mg L^{-1}) between 30 and 55 m depth. They followed a similar pattern of the thermoclines: surface concentrations quickly decreased between 30 and 35 m (Figs. 5-7), although, at the coastal stations St 34 (LC), the oxycline was found at about 22 m depth, and at around 15 m at St 42 (ACA) (Figs. 7b, e).

Nutrient concentrations and distributions are represented by nitrate, which may modulate the distribution of phytoplankton. In general, nitrate low concentrations (0.02 μM) were found in the surface layer (up to 30 m depth), but a strong nitratecline was detected between 18 and 30 m depth in most stations (Figs. 5-7). Nitrate concentrations considerably increased (up to 26.87 μM) deeper than 30 m depth. No clear pattern was found in the horizontal and latitudinal distribution.

Fluorescence (Chl-*a*) showed a general pattern with higher values (up to 7 mg m^{-3}, St 31) at coastal stations (St 5, 31, 34, and 42) than at more remote, oceanic stations in all transects studied (Figs. 2, 4-7, 9). In the ACA transect, fluorescence followed the temperature pattern (Fig. 4i, j), providing more evidence of the weak upwelling there. The previously detected pattern of SCM occurring in all stations was also found regarding vertical distribution. However, coastal stations (St 5, 23, 31, 34 and 42) had this feature shallower (15-25 m depth) than in more oceanic stations (St 9, 20a, 28a, 38a and 46a), where these SCM were found between 32 and 45 m (Figs. 5-7, 9). Many stations also showed the presence of DCM, especially the oceanic stations, located between 85 and 95 m deep (Figs. 5-7, 9). The highest Chl-*a* values were found at St 8 (Fig. 4b).

Phytoplankton structure in Cabo Corrientes

Bottle samples analyzed by microscopy yielded information on species composition, cell abundances (Table 1), and distribution (especially the vertical distribution). Cell densities ranged from 1.19 to 34.63 cells×10^4 L^{-1} (at St 5, 83 m, and St 7, 31 m, respectively), with no clear differences among densities in coastal or oceanic stations; in fact, higher densities were detected in St 7 (an intermediate one, with more than 2000 m depth). These densities were distributed similarly to the fluorescence and Chl-*a* profiles, and the highest abundances' peaks coincided with the SCM's depth (Figs. 5-7, 9).

The communities comprised up to 54 taxa (most identified at the species level). They were dominated by diatoms regarding species richness, where *Chaetoceros socialis* and other *Chaetoceros* spp., *Cylindrotheca*

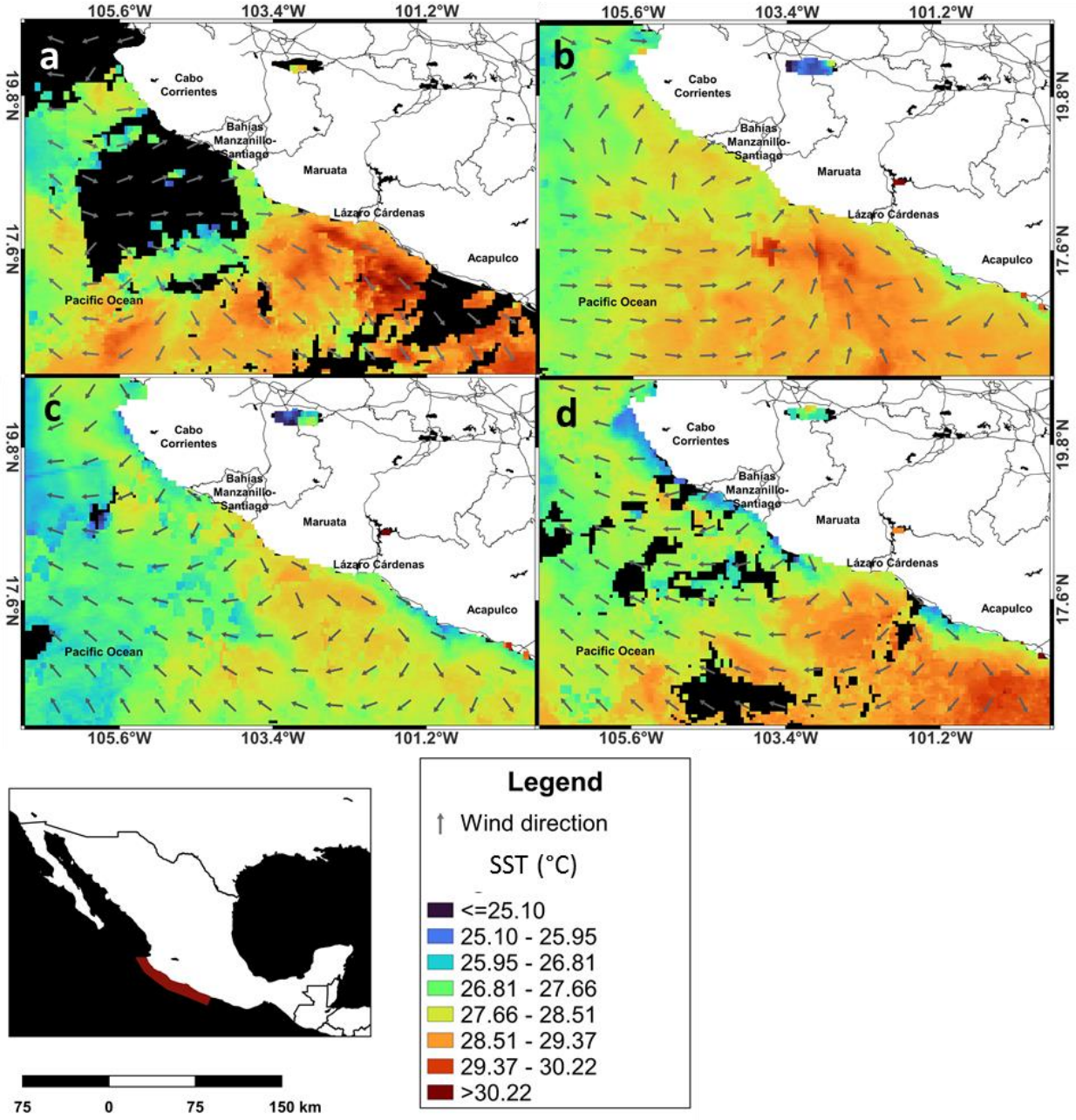

Figure 3. Wind map showing the direction of the wind and the spatial and temporal patterns of remote sensed Sea surface temperature (SST) of the study area for four different days in April 2013: a) April 1, 2013, b) April 5, 2013, c) April 8, 2013, and d) April 10, 2013.

closterium, *Eucampia cornuta*, *Guinardia delicatula*, and *Pseudo-nitzschia delicatissima* were the most abundant species (Table 1), with slight differences in composition among the three stations (5, 7 and 9). *Chaetoceros socialis* and other *Chaetoceros* spp. reached considerable abundances of up to 18 cells×10^4 L^{-1} at St 5, 20 m depth. The composition also included low densities of thecate dinoflagellates, unidentified athecate dinoflagellates, silicoflagellates, and cryptophytes (Table 1).

Picophytoplankton features

Results from flow cytometry showed the presence and abundance of three main picophytoplankton groups: *Synechococcus*, *Prochlorococcus*, and eukaryotes. *Synechococcus* densities varied from 0.15 to 9.56

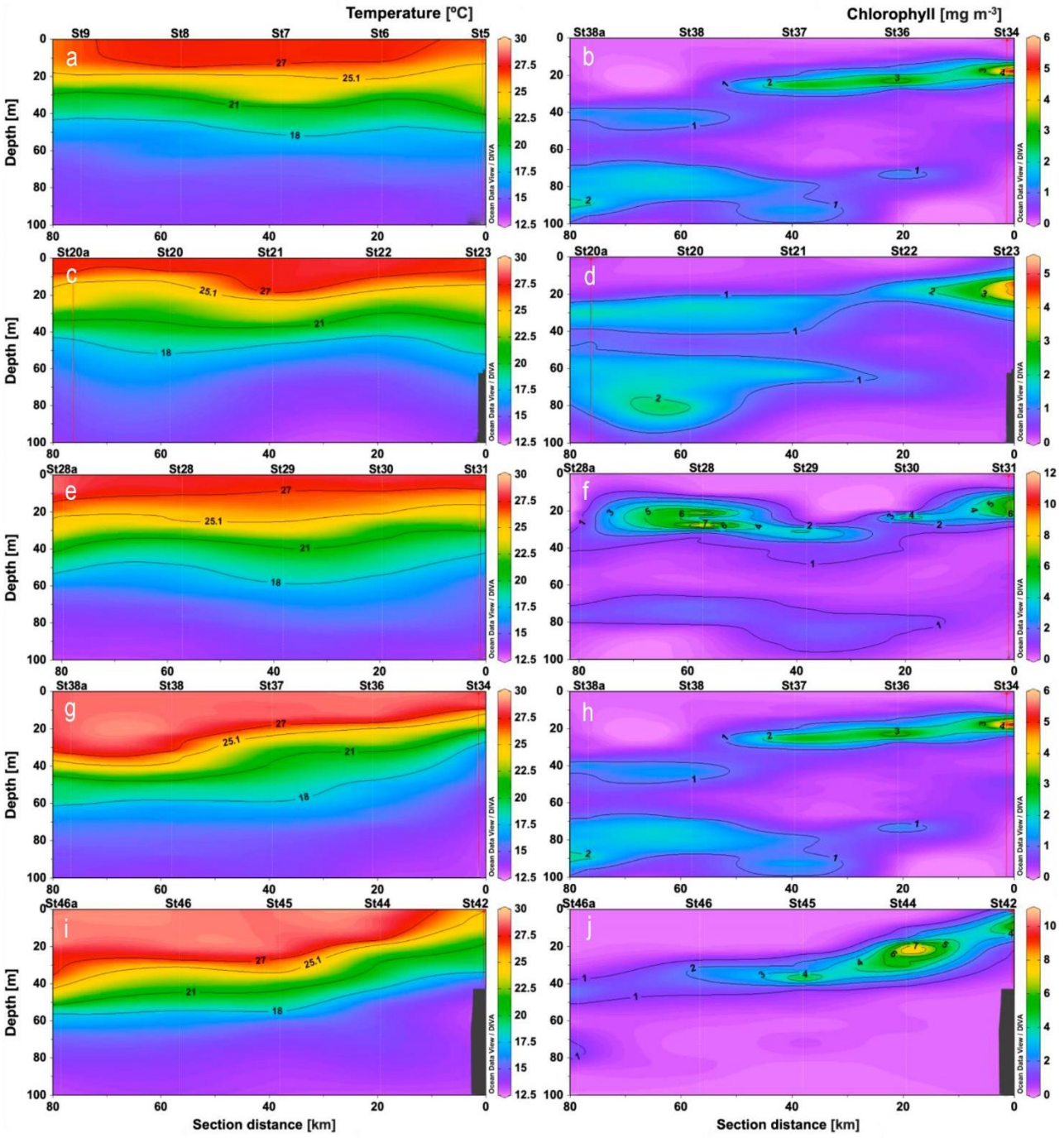

Figure 4. Distributions of temperature (left panel) and chlorophyll-*a* (right panel) in the transects of a-b) Cabo Corrientes, c-d) Bahías Manzanillo-Santiago, e-f) Maruata, g-h) Lázaro Cárdenas, and i-j) Acapulco.

cells×10^4 mL^{-1}, whereas *Prochlorococcus* abundances ranged from 0.05 to 21.7 cells×10^4 mL^{-1}, and picoeukaryotes varied from 0.01 to 4.75 cells×10^4 mL^{-1} (Table 2). Although the numerical abundances of *Prochlorococcus* were the highest, in terms of biomass, as expected, picoeukaryotes were more important. They contributed more, with values reaching up to 47.95 µg C L^{-1} (St 28a, 5 m). In contrast, the maxima values for *Synechococcus* and *Prochlorococcus* were 10.71 µg C L^{-1} (St 28a, 20 m) and 12.15 µg C L^{-1} (St 38, 85 m), respectively (Fig. 8).

Synechococcus and picoeukaryotes densities (and consequently in terms of biomass) appeared to be higher at the three northern zones, namely CC, BMS,

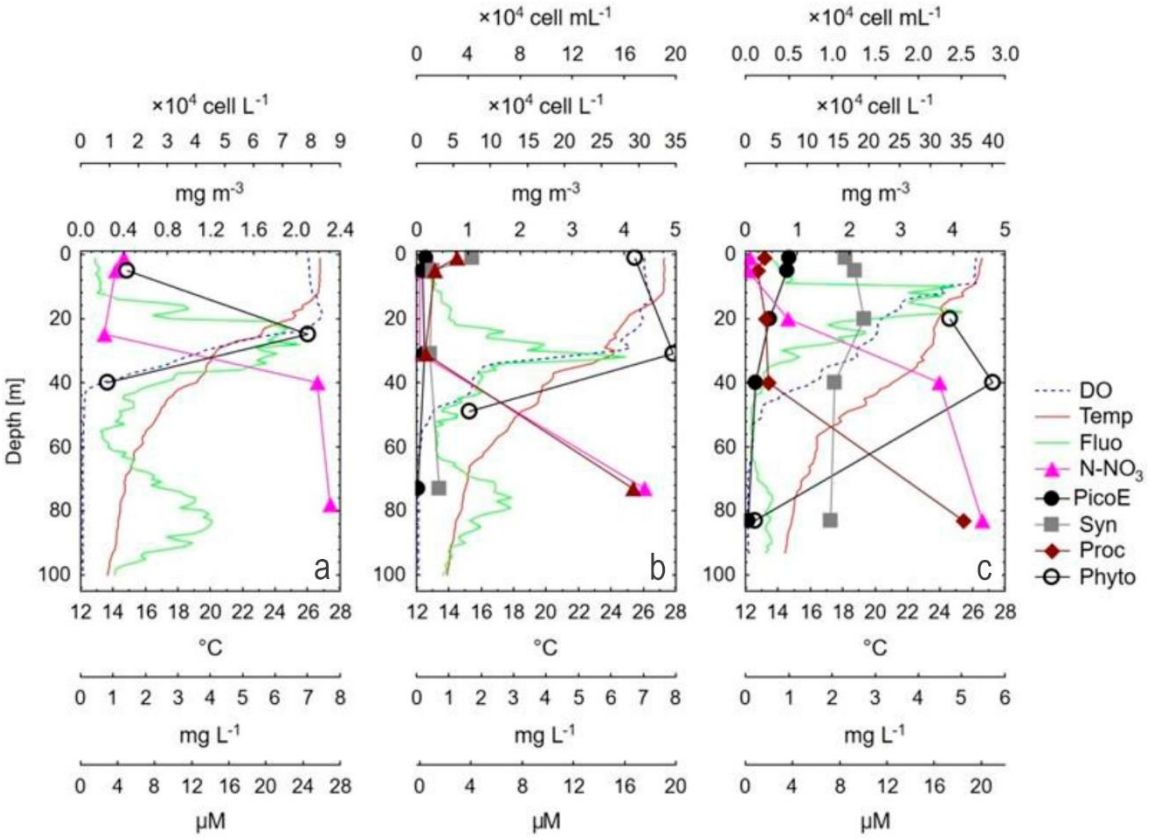

Figure 5. Vertical distribution of environmental variables (DO: dissolved oxygen, Temp: temperature, NO_3: nitrate), chlorophyll-*a*, three picoplankton different populations (Syn: *Synechococcus*, Pro: *Prochlorococcus*, and PicoE: Picoeukaryotes), and phytoplankton (Phyto) in stations of the Cabo Corrientes transect: a) station 9, b) station 7, c) station 5.

and MAR. In contrast, they diminished toward the southern zones, except for station 37 at 1 m depth (Figs. 5, 8). *Prochlorococcus* abundances were heterogeneous throughout the study area, with no considerable differences between coastal and oceanic stations. Still, at station 38a (an oceanic one, at 42 and 85 m depth), *Prochlorococcus* densities were higher than in the coastal station of that zone (LC) (Figs. 7-8). Picoeukaryotes densities were higher at station 28a at the surface (1-5 m depth) (Figs. 6, 8).

The vertical distribution of the abundances of these groups was fairly irregular, but some recurrent patterns were detected. *Synechococcus* abundances reached their highest values in coincidence with the SCM at stations 28a (20 m), 34 (18 m), 45 (38 m), and 46a (46 m) (Figs. 6-7). The highest *Prochlorococcus* abundances were in deeper layers, coinciding with the DCM, at stations 5 (83 m), 7 (73 m), 21 (61 m), 28a, 29 (85 m), 31 (75 m), 38a (85 m) and 46a (77 m) (Figs 4-7), and only in one station (45) its highest abundance was coincident with the SCM (Fig. 7). Picoeukaryotes followed the same pattern of *Synechococcus*, with abundance peaks coinciding with the SCM, or higher densities in surface and then decreasing with depth (St 21 and 42) (Figs. 6-7).

Photosynthetic phytoplankton pigments

Phytoplankton pigments measured yielded variable concentrations, with the most important and widely distributed pigments, fucoxanthin ranging from 0.004 to 1.50 µg L^{-1}, peridinin from 0 to 0.16 µg L^{-1}, 19' HF varied from 0 to 0.23 µg L^{-1}, zeaxanthin ranged from 0 to 0.11 µg L^{-1}, prasinoxanthin from 0 to 0.22 µg L^{-1} and divinyl Chl-*a* from 0 to 0.08 µg L^{-1} (Table 2). Other pigments such as alloxanthin, β-carotene, and Chl-*b* were detected occasionally or in very low concentrations and are partially shown (19' BF) (Table 2).

The highest concentrations of chlorophyll-*a* and most pigments (fucoxanthin, zeaxanthin, prasinoxanthin, and divinyl Chl-*a*) were found in coastal stations (St 5, 23, 31, 34, and 42) at different depths (Fig. 9), in most cases coinciding with the SCM, except

Table 1. List of species identified by microscopic analysis from stations 5, 7, and 9 in the Cabo Corrientes transect, including diatoms, dinoflagellates, silicoflagellates and Cryptophytes, with their maxima densities (cells L^{-1}).

Species	Max density (cells L^{-1})	Species	Max density (cells L^{-1})
Diatoms		*Navicula directa*	<1,000
Chaetoceros affinis	<1,000	*Planktoniella sol*	<1,000
Chaetoceros atlanticus	1,155	*Proboscia alata*	1,924
Chaetoceros brevis	<1,000	*Pseudo-nitzschia delicatissima*	26,554
Chaetoceros compressus	3,079	*Pseudo-nitzschia pungens*	13,470
Chaetoceros curvisetus	31,557	*Pseudo-nitzschia roundii*	1,924
Chaetoceros dichaeta	1,539	*Pseudo-nitzschia subcurvata*	<1,000
Chaetoceros didymus	<1,000	*Rhizosolenia acuminata*	<1,000
Chaetoceros laciniosus	<1,000	*Rhizosolenia bergonii*	<1,000
Chaetoceros lorenzianus	4,618	*Rhizosolenia imbricata*	<1,000
Chaetoceros pseudocurvisetus	30,788	*Rhizosolenia setigera*	<1,000
Chetoceros rostratus	<1,000	*Skeletonema pseudocostatum*	<1,000
Chaetoceros socialis	96,211	*Thalassionema nitzschioides*	6,927
Climacodium frauenfeldianum	<1,000	*Thalassiosira lineata*	<1,000
Cylindrotheca closterium	59,651	*Thalassiosira* sp.	4,618
Dactyliosolen phuketensis	<1,000	**Dinoflagellates**	
Detonula pumila	<1,000	*Alexandrium tamiyavanichii*	<1,000
Ditylum brightwellii	<1,000	*Amphidinium* sp.	1,924
Eucampia cornuta	47,721	*Dinophysis fortii*	<1,000
Guinardia delicatula	46,181	*Gymnodinium catenatum*	<1,000
Guinardia flaccida	12,315	*Gymnodinium* sp.	2,181
Guinardia striata	<1,000	*Gyrodinium* sp.	5,773
Haslea wawrikae	<1,000	*Heterocapsa* sp.	15,394
Hemiaulus hauckii	8,467	*Karenia* sp.	<1,000
Hemiaulus membranaceus	2,309	*Prorocentrum minimum*	<1,000
Leptocylindrus danicus	15,394	*Scrippsiella trochoidea*	<1,000
Leptocylindrus mediterraneus	10,391	**Silicoflagellates**	
Leptocylindrus minimus	15,394	*Octactis octonaria*	<1,000
Lioloma sp.	<1,000	**Cryptophytes**	<1,000

St 42, a shallow and eutrophic coastal station, where maxima values occurred close to surface (between 5 and 10 m depth). Fucoxanthin, mostly considered an indicator of the presence and relative abundance of diatoms, had considerable concentrations at coastal stations (Fig. 9). At St 45, an intermediate station, more oceanic than coastal, fucoxanthin reached 0.97 μg L^{-1} at 38 m depth, in coincidence with the SCM.

The vertical distribution of the pigments generally followed that of the Chl-*a* and fluorescence profiles, especially fucoxanthin and zeaxanthin, with the highest concentrations (peaks) coinciding with the SCM, except zeaxanthin at St 29, where its peak was located at 85 m, in coincidence with the DCM. As expected, divinyl Chl-*a* showed its highest concentrations at the DCM in the most remote oceanic stations (St 20a, 28a, 38a, and 46a). In St 7, it showed two peaks, at 19 and 73 m depth (Fig. 9). Concentrations of various pigments (4 or 5) peaked together in subsurface (between 18 and 40 m depth) at stations 5, 20a, 21, 28a, 31, 34 and 37 (Fig. 9).

Values of some pigments were significantly associated with the abundance of picophytoplankton, such as prasinoxanthin with picoeukaryotes (r = 0.30, P < 0.10) and divinyl Chl-*a* and Chl-*b* with *Prochlorococcus* (r = 0.48, P < 0.05 and r = 0.60, P < 0.05, respectively).

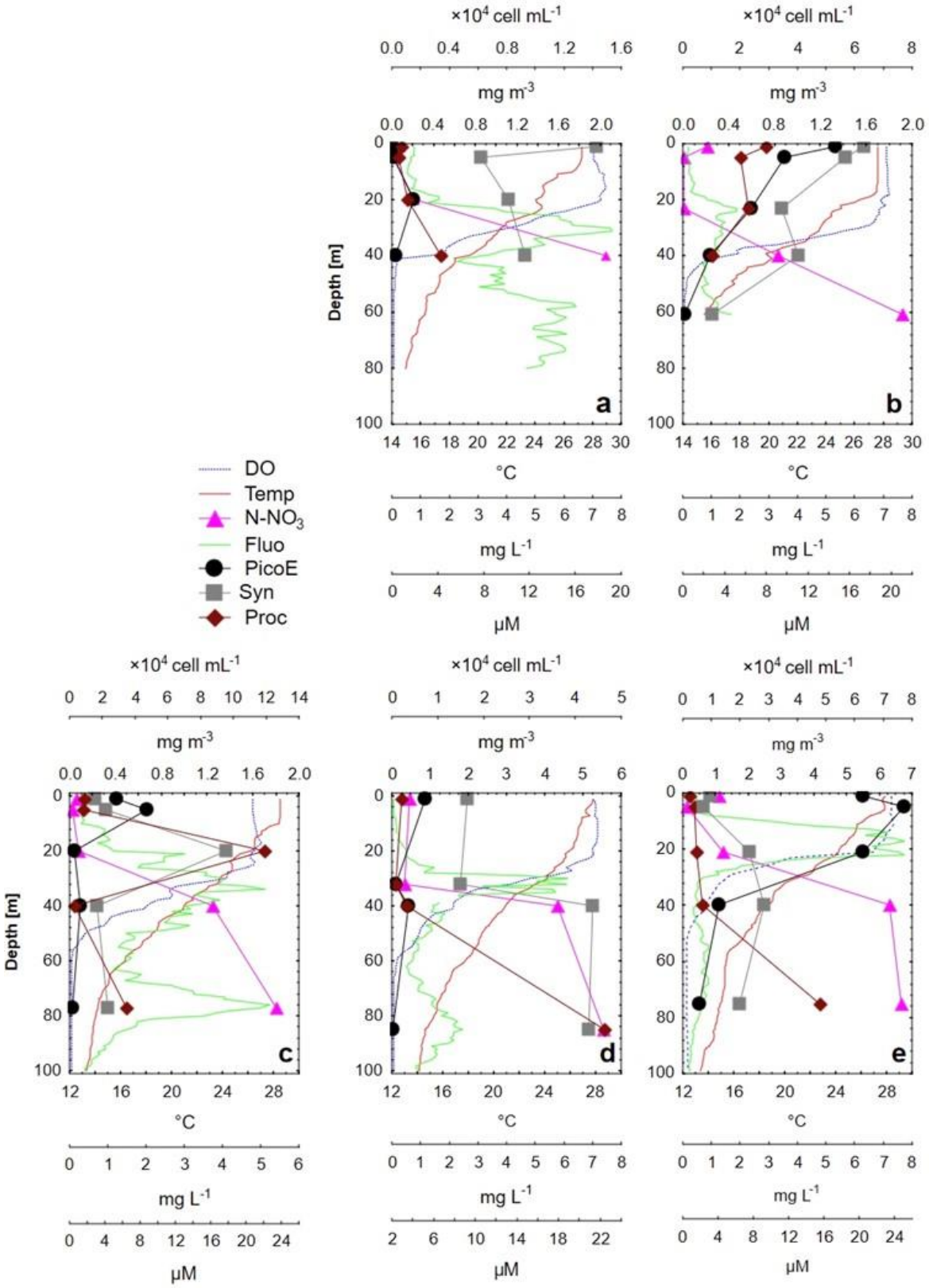

Figure 6. Vertical distribution of environmental variables (DO: dissolved oxygen, Temp: temperature, NO_3: nitrate), chlorophyll-*a*, and three picoplankton different populations (Syn: *Synechococcus*, Pro: *Prochlorococcus*, and PicoE: Picoeukaryotes) in stations of the Bahías Manzanillo-Santiago transect: a) station 20a, b) station 21, and Maruata transect: c) station 28a, d) station 29, e) station 31.

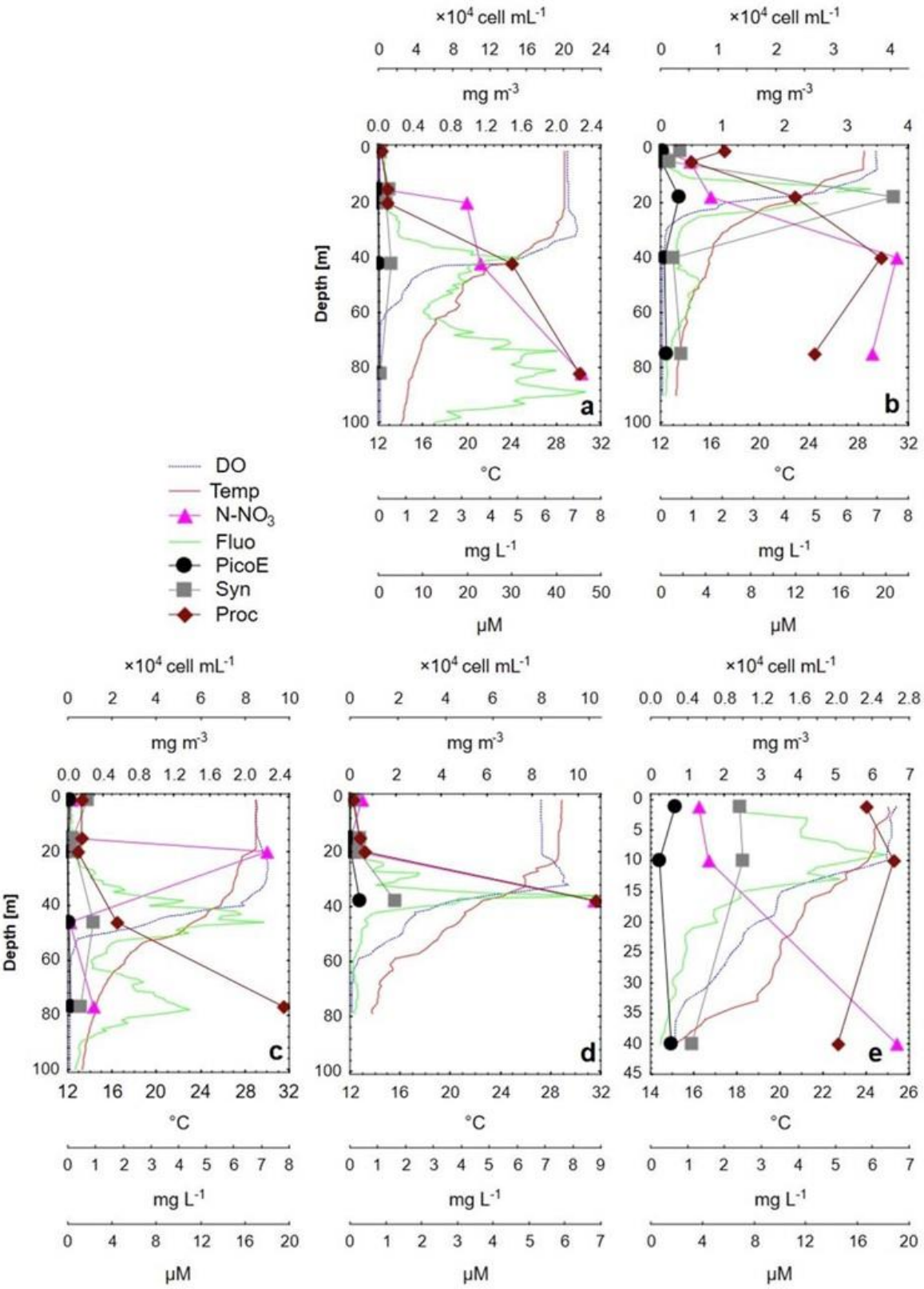

Figure 7. Vertical distribution of environmental variables (DO: dissolved oxygen, Temp: temperature, NO_3: nitrate), chlorophyll-*a*, and three picoplankton different populations (Syn: *Synechococcus*, Pro: *Prochlorococcus*, and PicoE: Picoeukaryotes) in stations of the Lázaro Cárdenas transect: a) station 38a, b) station 34, and Acapulco transect: c) station 46a, d) station 45, e) station 42.

Table 2. Picophytoplankton abundances and pigment concentrations of the study area during the oceanographic cruise "MareaR V". SD: standard deviation.

Variable	Cabo Corrientes (CC)		Manzanillo (BMS)		Maruata (MAR)		Lázaro Cárdenas (LC)		Acapulco (ACA)	
	Mean	SD	Mean	SD	Mean	SD	Mean	SD	Mean	SD
Abundance ($\times 10^4$cells mL^{-1})										
Synechococcus	1.568	0.992	1.669	1.288	2.7	2.24	1.287	1.742	0.707	0.499
Prochorococcus	2.543	5.085	1.015	1.946	2.08	3.28	4.499	6.962	2.673	3.536
Picoeukaryote	0.353	0.239	0.419	0.42	0.86	1.32	0.357	0.927	0.108	0.127
Concentration (μg L^{-1})										
Chlorophyll-*a*	0.124	0.194	0.101	0.153	0.09	0.18	0.043	0.086	0.161	0.248
Divinyl-chlorophyll-*a*	0.003	0.009	0.003	0.011	0	0.01	0.003	0.008	0.014	0.026
Total chlorophyll	0.127	0.194	0.104	0.152	0.1	0.18	0.045	0.086	0.175	0.273
Peridinine	0.024	0.055	0.007	0.014	0	0.01	0.007	0.01	0.016	0.025
19'-BF	0.001	0.004	0	0.001	0	0	0.002	0.007	0.01	0.023
Fucoxanthin	0.15	0.26	0.106	0.209	0.11	0.28	0.052	0.139	0.312	0.509
Prasinoxanthin	0.035	0.041	0.044	0.046	0.03	0.04	0.029	0.047	0.051	0.068
19'-HF	0.018	0.031	0.015	0.031	0.01	0.03	0.005	0.017	0.025	0.059
Zeaxanthin	0.037	0.033	0.038	0.028	0.03	0.02	0.032	0.02	0.054	0.026

Phytoplankton size fractions and pigment indices and ratios

The structure of phytoplankton size fractions estimated from the photosynthetic pigments showed that the nanoplankton fraction contributed the lowest proportion in the study area with ~5% (Table 3, Fig. 10). At the zones of MAR and ACA, micro- and picoplankton fractions contributed in about the same proportion (43-47%). In contrast, in BMS and LC, the microplankton fraction was dominant in the community (~50 and 60%, respectively). Microphytoplankton was more important (~58%) in the CC zone (Table 3, Fig. 10). At coastal stations (St 5 at CC, St 23 at BMS, St 31 at MAR, St 34 at LC, and St 42 at ACA) microphytoplankton was the major contributor (Fig. 10).

The pigment indices photoprotective carotenoids (PPC) to total pigments and photosynthetic carotenoids (PSC) to total pigments showed an apparent horizontal pattern in their distribution, corresponding with the environmental conditions: the highest values of PSC_{TP} were recorded at coastal stations of each transect (St 5 at CC, St 23 at BMS, St 31 at MAR, St 34 at LC, and St 42 and 45 at ACA) (Fig. 11), within the euphotic zone. Contrastingly, the photoprotection index (PI) increased in the direction coast to the ocean, reaching its highest values at more oceanic stations of the transects CC (St 9), MAR (St 20) and LC (St 28a) (Fig. 11).

The ratio PPS:PSC was close to 1, with natural deviations associated with areas of high productivity, particularly at St 5 (20 m), St 23 (18 m), St 31 (21 m), St 34 (18 m), St 42 (5 and 10 m), and St 45 (38 m), most of them within the coastal zone of each transect (except station 45).

Statistical analyses

The PCA revealed that the two first components explained 72.5% of the total variance (Fig. 12). temperature and dissolved oxygen were positively associated with the first component, which explained 65.6% of the variance. In contrast, phosphates and nitrates were negatively associated, suggesting the influence of upwelling (Fig. 12). Chl-*a* and ammonium were negatively associated with the second component, the zone of high biological activity. Nanoplankton fraction and *Prochlorococcus* biomass were positively correlated with the first component, whereas the PSC index and microplanktonic fraction were associated with the second component; the most coastal stations of each transect were grouped (top left quadrant), indicating the major productivity areas (Fig. 12).

DISCUSSION

Hydrographic and oceanographic conditions

Hydrographic and oceanographic conditions found in this study are common for spring in the region, inclu-

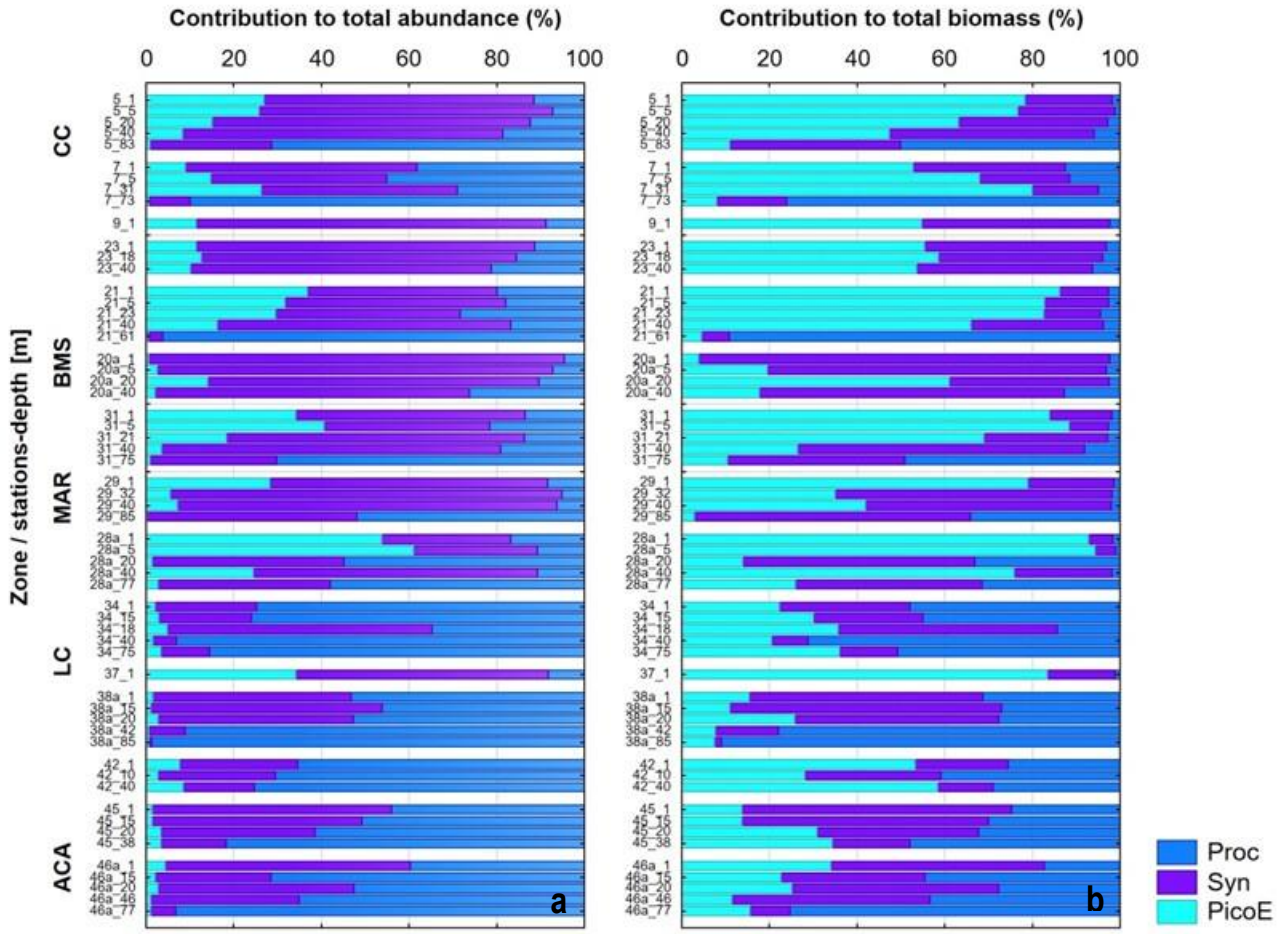

Figure 8. Contributions (%) of three picophytoplankton populations to a) abundance and b) biomass per station and depth (numbers are each station and depth, m), and transect. ACA: Acapulco, LC: Lázaro Cárdenas, MAR: Maruata, BMC: Bahías Manzanillo-Santiago, CC: Cabo Corrientes, Proc: *Prochlorococcus*, Syn: *Synechococcus*, PicoE: Picoeukaryotes.

ding the latitudinal thermal gradient from north to south (Gallegos et al. 2006, López-Sandoval et al. 2009, Pelayo-Martínez et al. 2017, Santana-Vega et al. 2018, Pajares et al. 2020). Relative thin mixed column water usually appeared in most northern zones (CC), and these layers increased their thickness towards the south. In contrast, the surface temperatures are higher in most southern zones (ACA), which confirms the latitudinal thermal gradient. The sudden decrease in the dissolved oxygen concentration and the oxycline depth are also characteristic features of the study area located within an OMZ (Maske et al. 2019).

Although we expected the presence of spring upwellings in the study area, especially CC, these most possibly occurred after the sampling dates (April 10, 2013) (Fig. 3d). The wind maps led us to observe some additional events, most of them showing possible upwellings, particularly at a zone between LC and ACA, because the persistence of the direction of the winds (Figs. 3b-d). However, when we sampled CC, the water column appeared more stratified, in contrast with the most southern zone, ACA, which showed conditions suggesting a weak upwelling, as the isotherm of 24°C was found between 18 and 22 m depth in a coastal station (St 42, ACA), and also supported by the gradual ascent of the Chl-*a* values in that transect and the high surface Chl-*a* concentration at St 42 (Figs. 4i-j, 7e), a novelty in the series of studies previously done in the study area.

The finding of DCM, located between 65 and 120 m depth, in more oceanic, remote locations, in addition to the usual SCM, is another interesting and important characteristic of the study area (Cepeda-Morales et al. 2009, Hernández-Becerril et al. 2018, Santana-Vega et al. 2018, Márquez-Artavia et al. 2019). These DCM are persistent in the OMZ of the Mexican Pacific between

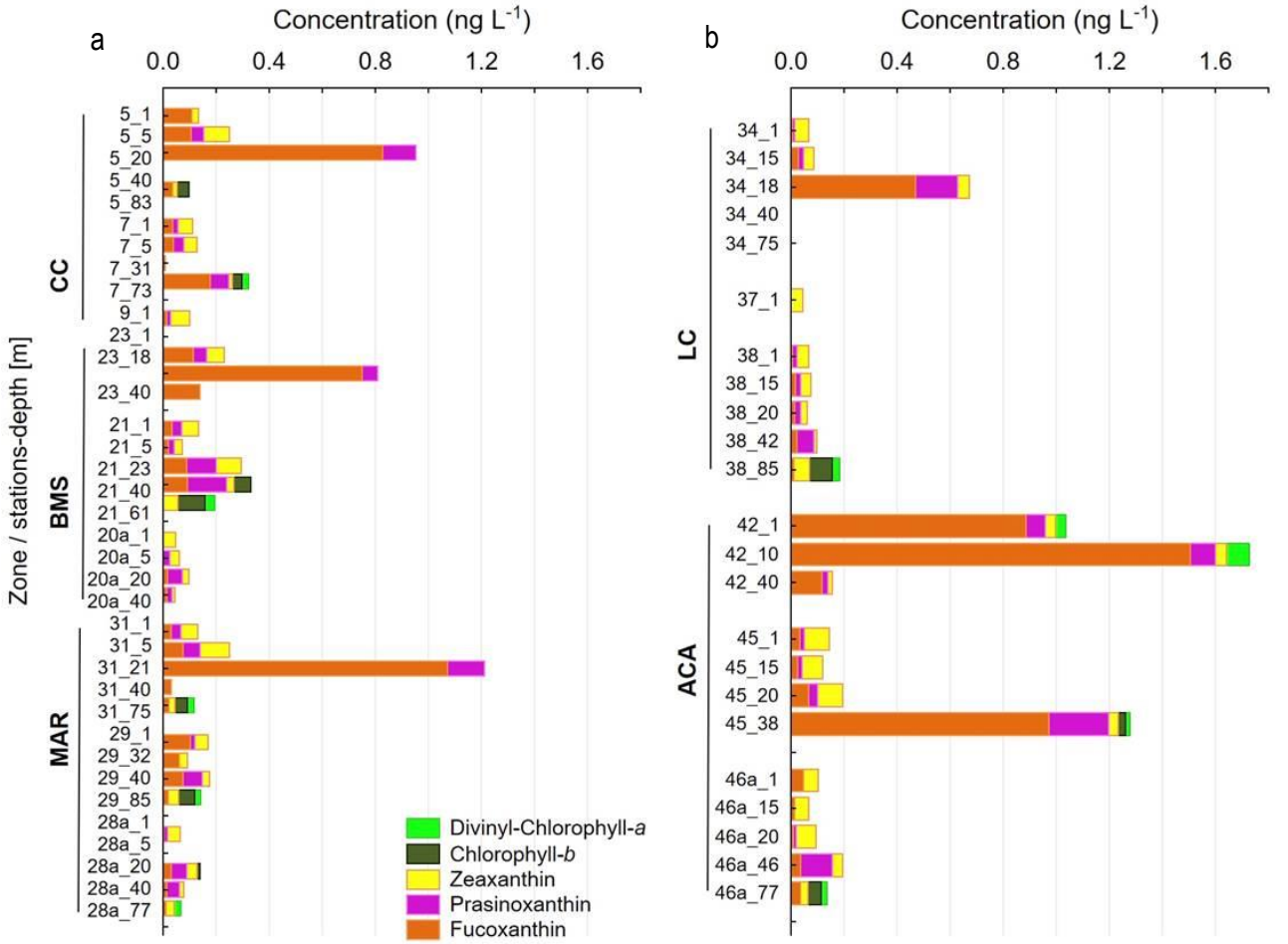

Figure 9. Vertical distribution of the major pigments at stations of each transect. Numbers are each station and depth (m). a) Stations in transects Cabo Corrientes (CC), BMS (Bahías Manzanillo-Santiago), and Maruata (MAR). b) Stations in transects Lázaro Cárdenas (LC) and Acapulco (ACA).

40 and 190 m, related to the subtropical subsurface water, which is nearly unaffected by mixing with other water masses (Márquez-Artavia et al. 2019).

Whereas the SCM are formed and maintained by a range of interacting processes, including enhanced phytoplankton growth under an optimal combination of light and nutrients, physiologically controlled swimming behavior or buoyancy regulation, and photoacclimation of pigment content, all influenced by food web interactions and hydrodynamics (Cullen 2015), the mechanisms which are involved in forming and maintaining the DCM are not completely understood. These mechanisms may include particular conditions of the deeper water layers in the study area (and OMZ all over the world), with very low (suboxic) dissolved oxygen concentrations, low light intensity (with a spectral blue feature), and high nitrate concentrations. All of them may favor the formation of a second, deep fluorescence maximum, especially in oceanic areas that are associated with high *Prochlorococcus* populations (Goericke et al. 2000). The DCM has been reported to occur at irradiances ranging from 0.2 to 2% of surface values (Goericke et al. 2000).

Phytoplankton and picophytoplankton structure

The phytoplankton's structure at CC stations (the most northern zone) was studied by microscopic analysis (Table 1) and photosynthetic pigments. The cell densities of phytoplankton were relatively low to moderately high (1.19 to 34.63 cells×10^4 L^{-1}), especially if compared with reports of other years in the same area for about the same period of the year, where a high average value may be 6.89 cells×10^5 L^{-1} and up to 2.31 cells×10^6 L^{-1}, when blooms conditions were found (Hernández-Becerril & Vega-Juárez 2022).

Table 3. Various pigment indices values from the study area during the "MareaR V" oceanographic cruise. SD: standard deviation; Min: minimum; Max: maximum.

Pigments/Index		Cabo Corrientes (CC)				Manzanillo (BMS)				Maruata MAR)				Lazaro Cardenas (LC)				Acapulco (ACA)			
		Mean	SD	Min	Max	Mean	SD	Min	Max	Mean	SD	Min	Max	Mean	SD	Min	Max	Mean	SD	Min	Max
Total chlorophyll *a*	TChl a	0.13	0.19	0	0.63	0.1	0.15	0	0.57	0.1	0.18	0.02	0.71	0.06	0.09	0	0.3	0.18	0.27	0.02	0.92
Photoprotective carotenoids	PPC	0.04	0.03	0	0.1	0.04	0.03	0	0.1	0.04	0.03	0	0.11	0.04	0.02	0.01	0.08	0.06	0.03	0.02	0.1
Total diagnostic pigments	DP	0.24	0.3	0.01	0.98	0.18	0.24	0.03	0.91	0.19	0.32	0.03	1.23	0.13	0.19	0.04	0.62	0.42	0.58	0.07	1.79
Total accessory pigments	Tacc	0.3	0.39	0.01	1.29	0.23	0.32	0.04	1.2	0.25	0.41	0.05	1.61	0.17	0.25	0.04	0.83	0.56	0.79	0.08	2.41
Photosynthetic pigments	PSC	0.32	0.5	0.01	1.61	0.23	0.4	0	1.48	0.25	0.51	0.03	1.95	0.14	0.28	0	0.88	0.54	0.86	0.03	2.67
Total pigments	TP	0.43	0.58	0.01	1.92	0.34	0.47	0.04	1.78	0.35	0.6	0.09	2.32	0.22	0.35	0.04	1.13	0.73	1.06	0.1	3.33
Photoprotection index	PI	0.17	0.18	0	0.63	0.15	0.14	0.03	0.57	0.15	0.18	0.05	0.71	0.1	0.1	0.02	0.34	0.23	0.27	0.08	0.98
Total chlorophyll *a* to total pigments	T $Chla_{TP}$	0.24	0.1	0	0.35	0.29	0.1	0	0.39	0.31	0.12	0.15	0.55	0.22	0.11	0	0.41	0.23	0.05	0.12	0.34
Photoprotective carotenoids to total pigments	PPC_{TP}	0.2	0.21	0	0.6	0.29	0.23	0	0.8	0.23	0.15	0	0.54	0.4	0.28	0.04	1	0.3	0.26	0.02	0.7
Photosynthetic carotenoids to total pigments	PSC_{TP}	0.42	0.27	0.12	1	0.25	0.18	0	0.53	0.28	0.18	0.05	0.53	0.23	0.17	0	0.51	0.32	0.19	0.08	0.57
Total accessory pigments to total pigments	$TAcc_{TP}$	0.76	0.1	0.65	1	0.71	0.1	0.61	1	0.69	0.12	0.45	0.85	0.78	0.11	0.59	1	0.77	0.05	0.66	0.88
PPS:PSC ratio	PPC:PSC	1.08	1.67	0	5.23	0.75	0.55	0	1.43	2.06	3.17	0	11.56	2.27	2.21	0.07	6.66	2.04	2.7	0.03	9.09
Picophytoplankton proportion	Ppf	58.52	27.12	16.05	100	40.73	32.3	0	100	44.15	28.93	7.96	100	36.8	26.98	0	80.42	47.53	28.45	9.91	86.76
Nanophytoplankton proportion	Npf	4.47	5.42	0	12.46	6.85	7.23	0	19.3	7.26	11.48	0	40.95	1.42	4.25	0	12.74	5.07	7.82	0	25.7
Microphytoplankton proportion	Mpf	35.97	30.7	0	83.95	50.84	32.34	0	100	42.93	27.41	0	92.04	60.1	28.11	6.84	100	45.27	32.93	2.13	90.09

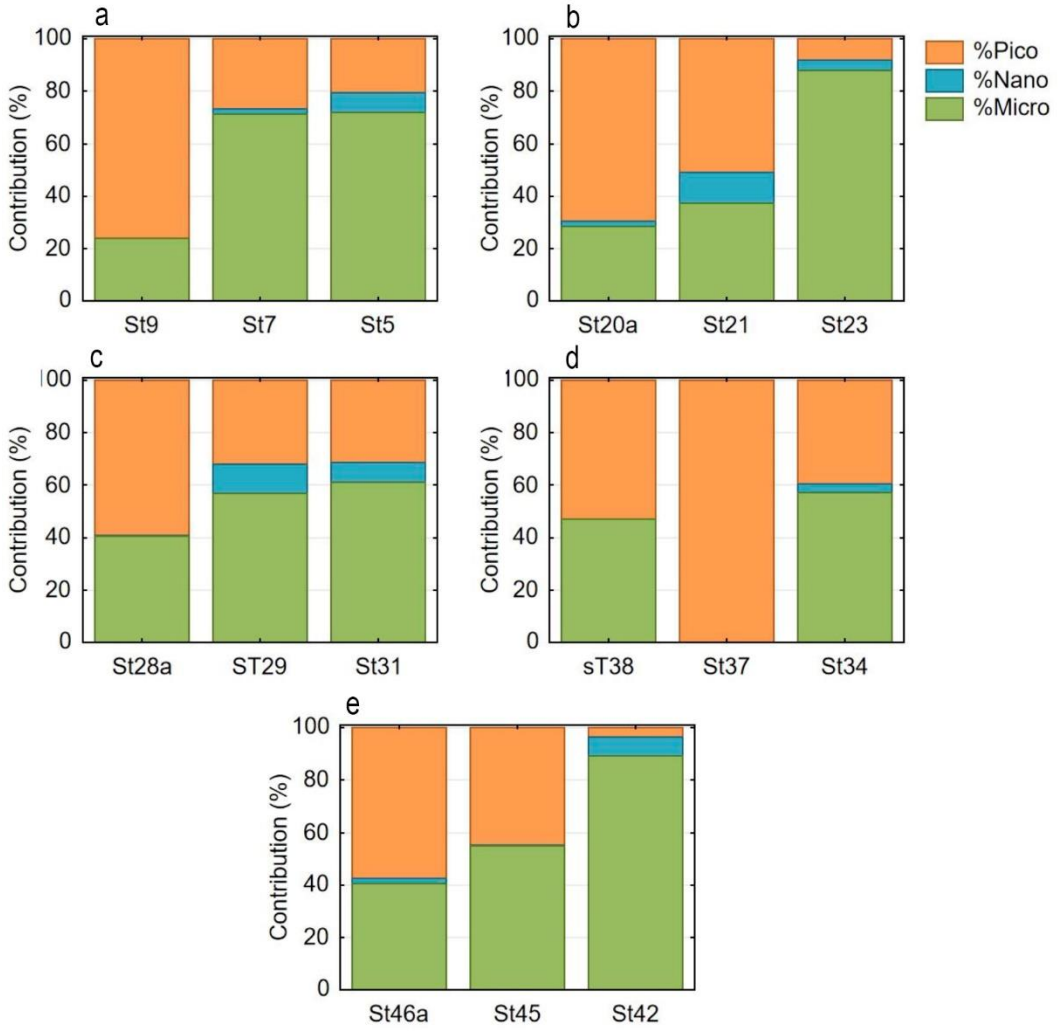

Figure 10. Phytoplankton size fractions (%) were estimated using photosynthetic pigments per station and transect. a) Transects Cabo Corrientes, b) Bahías Manzanillo-Santiago, c) Maruata, d) transects Lázaro Cárdenas, e) Acapulco. Pico: picoplankton. Nano: nanoplankton, Micro: microplankton.

Despite the relative stratification of stations in CC, diatoms were the most abundant taxonomic group, as confirmed by high concentrations of fucoxanthin. The species composition also included a few unidentified athecate photosynthetic dinoflagellates (*Gymnodinium* and *Karenia* species), silicoflagellates, and small cryptophytes (Table 1). Expectably, the phytoplankton densities coincided with the patterns of Chl-*a* in all three stations, peaking also together at the SCM (Figs. 5-7, 9).

The numerical predominance of diatom species, which were mainly chain-forming: *Chaetoceros socialis* and other *Chaetoceros* spp., *Eucampia cornuta*, *Guinardia delicatula*, as abundant species, but also including some *Pseudonitzschia* spp., and *Thalassionema nitzschioides* in fewer numbers (Table 1), is commonly found in coastal areas in this zone of the Mexican Pacific (Hernández-Becerril 1996, Esqueda-Lara et al. 2005, Vega-Juárez 2014).

Besides the diatom's important contribution to diversity and abundance at stations in the CC zone, we also found that fucoxanthin, as a signature pigment, was the most significant pigment in most samples of all stations, particularly in coastal stations (5, 23, 31, 34, and 42) and station 45 (an intermediate station) at 38 m. We have no information on microscopic analysis there. Generally, and expectably, all pigments analyzed yielded higher concentrations in coastal stations than in more oceanic ones (Fig. 9).

A previous paper on prokaryote picophytoplankton and its distribution along environmental gradients in the central Mexican Pacific showed similar characteristics

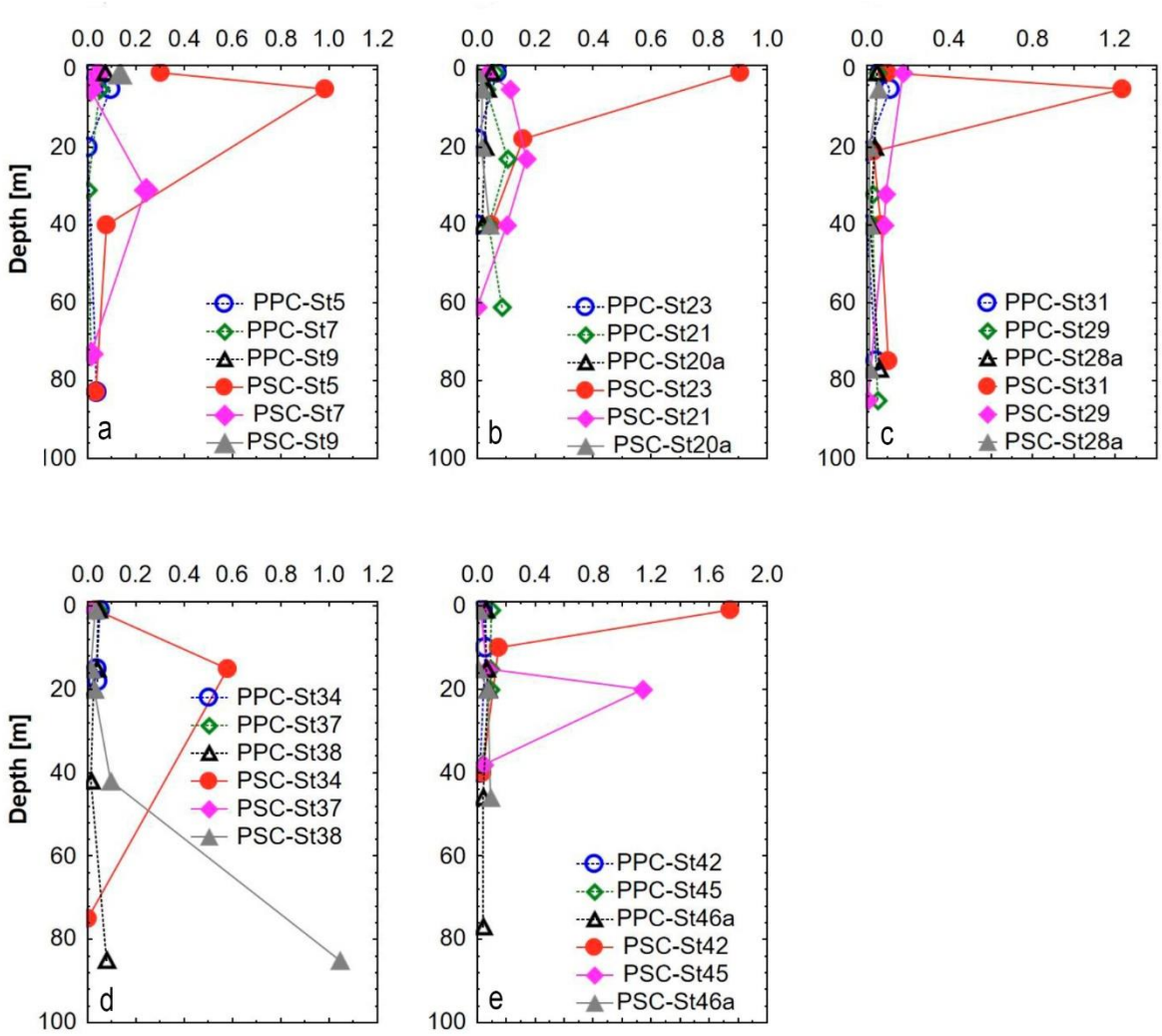

Figure 11. Vertical profiles of phytoplankton pigment indices in each station of the transects. a) Stations in transects Cabo Corrientes, b) stations in Bahías Manzanillo-Santiago, c) stations in Maruata, d) stations in transects Lázaro Cárdenas, e) stations in Acapulco. PSC: photosynthetic carotenoids, PCC: photoprotective carotenoids.

in this study (Santana-Vega et al. 2018). Differential geographic distribution of both *Synechococcus* and *Prochlorococcus* was already noticed. We also observed *Synechococcus* and picoeukaryotes densities (and consequently in terms of biomass), which appeared to be higher in three northern zones: CC, BMS, and MAR. In contrast, they diminished toward southern zones (Fig. 8). These data are consistent with previous observations in other marine subtropical areas where *Synechococcus* and autotrophic eukaryotes dominated mesotrophic waters. In contrast, *Prochlorococcus* dominated in more oligotrophic areas (Gérikas-Ribeiro et al. 2016).

We also recognized a unique feature occurring in OMZ concerning the vertical distribution of *Prochlorococcus*, which can reach high densities and aids in forming the DCM, thus contributing to the biomass and productivity in these important layers. The highest *Prochlorococcus* abundances and biomass are strongly related to the DCM, which were located between 65 and 95 m deep, and this fact confirms previous results (Santana-Vega et al. 2018, Márquez-Artavia et al. 2019) and the particular niche of an ecotype of *Prochlorococcus* adapted to inhabit in layers were the intensity of light is very limited (low light or LL ecotype, Rocap et al. 2002, Bibby et al. 2003). Furthermore, some particular *Prochlorococcus* ecotypes known as LLV and LLVI have only been found in OMZ (Lavin et al. 2010, Franz et al. 2012). More recently, Pajares et al. (2020) identified opera-

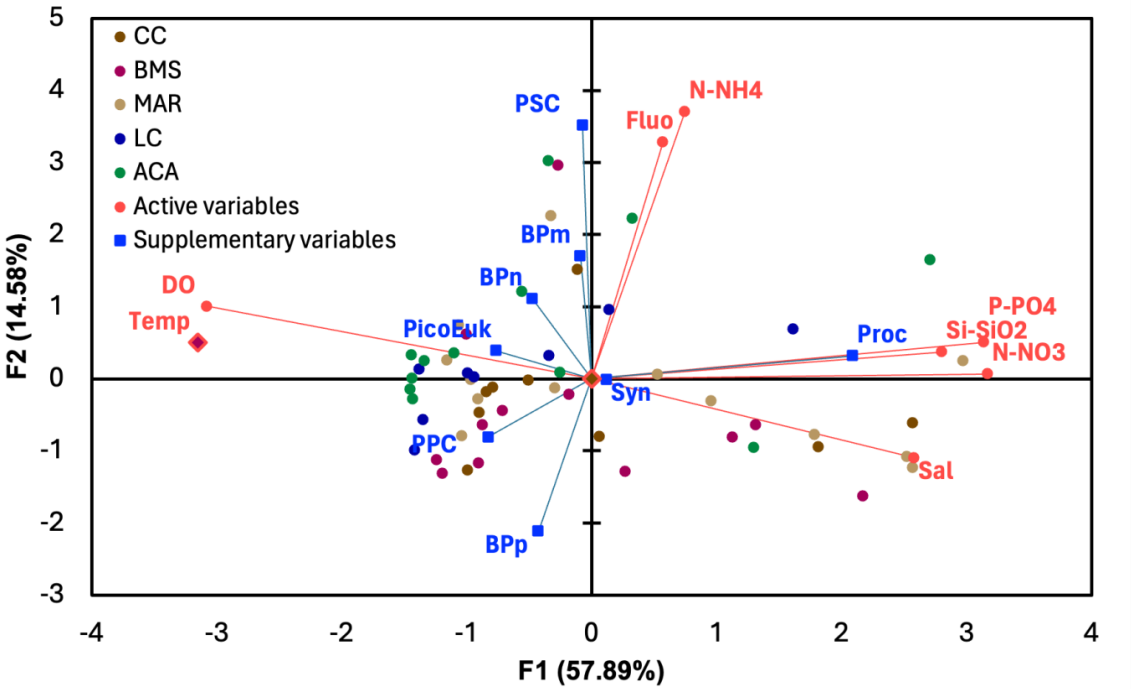

Figure 12. PCA biplot of the two first components from data of environmental and biotic variables of the central Mexican Pacific. Circles represent the samples, active variables are in red, and supplementary variables are in blue. CC: Cabo Corrientes, BMS: Bahías Manzanillo-Santiago, MAR: Maruata, LC: Lázaro Cárdenas and ACA: Acapulco.

tional taxonomic units of the *Prochlorococcus* ecotype MIT9313 (adapted to LL) distributed in depths similar to those of the DCM. This feature may also be an important characteristic of an area within an OMZ (Goericke et al. 2000). No changes in the oxygen concentration matched with high *Prochlorococcus* densities (Figs. 5-7).

The pigments zeaxanthin and divinyl Chl-*a*, characteristic of *Synechococcus* and *Prochlorococcus*, respectively, usually followed the vertical distribution of both picoprokaryotes, especially at the SCM, where zeaxanthin had relatively high concentrations, coinciding with higher *Synechococcus* abundances, and at the DCM, where both divinyl Chl-*a* and *Prochlorococcus* were concurrent in concentrations and abundances, respectively (Figs. 5, 7).

The eukaryote picophytoplankton fraction, generally poorly studied in the study area, followed general characteristics of previous papers in other areas of the world, with lower densities compared with the prokaryote compound and peaks of abundance at subsurface layers (Worden 2006, Worden & Not 2008, Hernández-Becerril et al. 2012b, Wang et al. 2019) (Figs. 5, 7). A previous paper provided information on the diversity of the eukaryotic fraction between 30 and 1.6 µm size in the study area (Duret et al. 2015), and more recently, picoeukaryotes abundance and distribution were assessed (Pajares et al. 2020).

It appeared that picoeukaryote abundance was in covariance with *Synechococcus* (r = 0.44), as shown in other parts of the world (Worden & Not 2008). However, the picoeukaryotes abundance did not increase with depth and was not associated with the DCM (Figs. 5, 7). Picophytoeukaryotes can contribute significantly to biomass and productivity (Fig. 8), even when at lower abundance than the picocyanobacteria (Worden & Not 2008), and it was also found in our results, where picoeukaryotes counted with higher biomass than picoprokaryotes (Fig. 8).

The combination of relatively high densities of picoeukaryotes determined by flow cytometry, with a consequent increase in biomass, and the presence and important concentrations of the pigment prasinoxanthin at certain points of the water column (prasinoxanthin and picoeukaryotes were positively and significantly related: $r = 0.30$, $P < 0.10$), strongly suggest that various world-wide picoplanktonic mamiellophytes, possessing prasinoxanthin (Latasa et al. 2004), should be well represented in the study area. Recent and preliminary metabarcoding information obtained from samples of the study area indicates that *Bathycoccus prasinos*, *Micromonas* sp., and *Ostreococcus taurii* are

within the list of taxa detected following that method (targeting at the V9 region of the SSU rDNA) (Hernández-Becerril et al. *in press*). This finding is not unexpected, as recent reports from many areas of the world seas indicate the relevance and important role of these picoplankton components (Cheung et al. 2010, Collado-Fabbri et al. 2011, Kirkham et al. 2013, Tragin et al. 2016). There is significant evidence which indicates that the Mamiellales are one of the more ecologically important picophytoeukaryote groups, especially in coastal waters (Not et al. 2004, Worden 2006, Worden & Not 2008, Hernández-Becerril et al. 2012b), and this fact may be also confirmed recently in open waters (Wang et al. 2019).

Employing other methods to assess the protist and phytoplankton diversity in OMZ, such as the use of molecular approaches, dinoflagellates (including Gymnodiniales, Syndiniales, and Gonyaulacales) were dominant in northern Chile, and the current study area, especially in mixed layers (Parris et al. 2014, Duret et al. 2015). In contrast, in Costa Rica, dinoflagellates were also dominant, especially Gymnodiniales, and diatoms and Eustigmatophyceae were important in surface layers, together with groups such as Raphidophyceae, Haptophytes and Prasinophytes (Mamiellophytes) (Jing et al. 2015).

Following the CHEMTAX approach, diatoms were the most dominant group in the phytoplankton in the upper 20 m of coastal upwelling areas, with Cryptophytes and Mamiellophytes being also important, dinoflagellates playing a negligible role in terms of biomass, Chlorophytes, Haptophytes, Chrysophytes and *Synechococcus* occurring in subsurface layers (0-30 m) in the inner shelf area, and *Prochlorococcus* (low-light adapted populations) also exhibiting differential coast-to-ocean and vertical distributions, with a marked deep peak at 80-90 m, at more oceanic stations, in the eastern tropical south Pacific (Perú) (Franz et al. 2012), whereas in the northeastern tropical Pacific (north to the current study area) the phytoplankton surface community included *Synechococcus*, *Prochlorococcus* and Haptophytes (Prymnesiophytes), with increase of diatoms and Chlorophytes at the SCM, and dinoflagellates, Cryptophytes and Mamiellophytes contributing less, and with a different contributions of the groups between surface and SCM (Miranda-Álvarez et al. 2020, Larios-Muñiz et al. 2022).

However, we should consider that both approaches may yield different results, as molecular tools may reveal "hidden" diversity, including groups and organisms, both photosynthetic and heterotrophs. In contrast, the CHEMTAX approach only considers photosynthetic phytoplankton, as the method's base is photosynthetic pigments.

The general phytoplankton (including picophytoplankton) structure shown here indicates that diatoms are the most abundant group of microphytoplankton at the coastal stations and subsurface, *Prochlorococcus* and *Synechococcus* show differences in distribution depending on distance from the coast and depth (possibly driven by temperature and light availability). *Prochlorococcus* is the main contributor of the DCM, compatible and almost identical with results in other parts of the world (González-García et al. 2018).

Phytoplankton size-fractions

According to the calculations, the microplankton fraction contributes more importantly (up to 58%) to the total phytoplankton community at the CC zone. In contrast, picoplankton was dominant in both BMS and LC zones, and the proportion was similar between pico- and microplankton in MAR and LC. The contribution of the nanoplanktonic fraction was very low (about 5%) (Table 3, Fig. 9). Microscopic analysis confirmed microplankton dominance at CC zone stations, with significant diatom densities. In contrast, picoplankton population densities in this zone were not high (Table 2).

The distribution of different, somehow contrasting phytoplankton structures may be due to the variable oceanographic conditions found among the whole study area, which include more stratified conditions (even changing at stations in the same transect) and weak upwelling conditions (particularly important at coastal stations) (Figs. 2-3) favoring small-size fractions or promoting larger phytoplankton cells, respectively (Ward et al. 2014, Marañon 2015). In certain stations, particular hydrographic conditions, from coastal stations to oceanic and remote stations, show ample possibilities for containing diverse communities, which may count to explain the variability of the phytoplankton communities, for some coastal environments may bear high concentrations of nutrients, more turbulence and less light penetration, contrasting with oceanic stations which may have low concentrations of nutrients and high light penetration.

Phytoplankton pigments indices

In general, the pigment index values of PPC gradually increased from the northern zones (CC) to the southern zones (ACA) (Fig. 10), which allows us to assume that phytoplankton accumulates these carotenoids to mitigate the effect of higher irradiance and ultraviolet radiation usually detected in more tropical areas (Barlow et al. 2007, Moreno et al. 2012).

The high pigment index values of PSC recorded at the coastal stations in BMS, MAR, LC, and ACA may be interpreted as an indicator of a relatively high productivity episode resulting from the upwelling conditions found and typical of the season (Gallegos et al. 2006, López-Sandoval et al. 2009). In contrast, the increase of the pigment index values of PPC at more oceanic stations (St. 9, 20a, 28a, and 46a) (Figs. 11-12) is associated with the dominance of the smallest phytoplankton fraction (Gibb et al. 2000). Under similar conditions, a poor-nutrient water column associated to low Chl-*a* concentration, the pico-phytoplankton was dominant (*Synechococcus* and *Prochlorococcus*) (Vieira-Araujo et al. 2017), resembling the spatial variation in stations 9 at CC, 20a at BMS and 28a at MAR.

Similarly, the low values of the PI obtained from the coastal stations of the study area are possibly due to the higher nutrient concentrations, mainly ammonium, and the mixing of the water column, which may favor the production of PSC (Rodríguez et al. 2006, Barlow et al. 2007), partially confirmed by the PCA analysis, where ammonium and Chl-*a* are related.

CONCLUSIONS

In this paper, we studied the structure of the phytoplankton in an OMZ, particularly focusing on the size fractions and the importance of the picoplankton fraction. We provide sufficient information to confirm the effect of the environmental gradients on the phytoplankton community: latitudinal and vertical gradients are evident in the study area, but longitudinal (coast to ocean) gradients may also be important. An unexpected weak upwelling was reported in most southern zones, including the ACA. We documented the co-dominance of the fractions pico- and microplankton, spatially differentiated due to the diverse hydrographic and oceanographic conditions: microplankton being more important at the CC zone, picoplankton dominant in both BMS and LC zones, and a similar proportion of pico- and microplankton at MAR and LC. Microplankton prevailed in coastal stations under conditions associated with mixed water columns, higher nutrient concentrations, and low light penetration, with diatoms as the dominant group.

In contrast, picoplankton was more important in oligotrophic, more oceanic areas, especially at the DCM related to oligotrophic and stratified water columns. We confirmed the importance of certain taxonomic groups, such as diatoms in the coastal zone and the SCM. In contrast, the picoprokaryote *Prochlorococcus* appears to be an important contributor in more oceanic zones and the DCM, and the picoplanktonic Mamiellophytes are suggested to be also an important and persistent component in the study area. The general picture with diatoms as the most abundant group of microphytoplankton at the coastal stations and subsurface, *Prochlorococcus* and *Synechococcus* showing differences in distribution depending on distance from the coast and depth, and *Prochlorococcus* as the main responsible of the DCM, is quite compatible and almost identical with results in other similar parts of the world.

ACKNOWLEDGMENTS

We are grateful to Sergio Castillo-Sandoval for the nutrient analysis performed. Many thanks to the R/V "El Puma" crew for their support and help during the oceanographic cruise "MareaR V". Partial support for this study was provided by PAPIIT, DGAPA, UNAM (Project IN296516), whereas Instituto de Ciencias del Mar y Limnología, UNAM, financed the publication of this paper. Coordinación de la Investigación Científica (CIC, UNAM) approved and supported the use of the R/V "El Puma" to carry out the oceanographic cruise "MareaR V". We thank an anonymous reviewer for raising interesting points and important suggestions.

Author contributions

DUHB: Material preparation, data collection, and analysis performed; writing, reviewing, editing, general supervision; FVC: Material preparation, data collection, and analysis performed; writing, reviewing, and editing; FJGM: Material preparation, data collection, and analysis performed; reviewing and editing; EJPM: Material preparation, data collection and analysis performed; reviewing; MMI: Material preparation, data collection and analysis performed; SABC: Material preparation, data collection and analysis performed; AUVR: Data collection and analysis performed.

Declaration of competing interest

The authors declare no potential conflict of interest in this manuscript.

REFERENCES

Band-Schmidt, C.J., Morquecho, L., Hernández-Becerril, D.U., Reyes-Salinas, A. & Bravo-Sierra, E. 2004. Raphidophyceans on the coasts of Mexico. Hydro-biologia, 515: 79-89. doi: 10.1023/B:HYDR.0000027320.00977.8b

Barlow, R., Kyewalyanga, M., Sessions, H., Van den Berg, M. & Morris, T. 2008. Phytoplankton pigments, functional types, and absorption properties in the Delagoa and Natal Bights of the Agulhas ecosystem. Estuarine, Coastal and Shelf Science, 80: 201-211. doi: 10.1016/j.ecss.2008.07.022

Barlow, R., Stuart, V., Lutz, V., Sessions, H., Sathyendranath, S., Platt, T., et al. 2007. Seasonal pigment patterns of surface phytoplankton in the subtropical southern hemisphere. Deep-Sea Research - Part I, 54: 1687-1703. doi: 10.1016/j.dsr.2007.06.010

Becerra-Reynoso, R. 2017. Distribución vertical, productividad primaria y análisis ecológico del fitoplancton marino en una zona de alta productividad en la costa de Tecpan de Galeana, Guerrero, México. Tesis de Licenciatura, Universidad Nacional Autónoma de México, Ciudad de México.

Bibby, T.S., Mary, I., Nield, J., Partensky, F. & Barber, J. 2003. Low-light-adapted *Prochlorococcus* species possess specific antennae for each photosystem. Nature, 424: 1051-1054. doi: 10.1038/nature01933

Cepeda-Morales, J., Beier, E., Gaxiola-Castro, G., Lavin, M.F. & Godínez, V.M. 2009. Efecto de la zona del mínimo de oxígeno en el segundo máximo de clorofila-*a* en el Pacífico oriental tropical mexicano. Ciencias Marinas, 35: 389-403.

Cheung, M.K., Au, C.H., Chu, K.H., Kwan, S.H. & Wong, C.K. 2010. Composition and genetic diversity of picoeukaryotes in subtropical coastal waters as revealed by 454 pyrosequencing. ISME Journal, 4: 1053-1059. doi: 10.1038/ismej.2010.26

Clarke, K.R. & Gorley, R.N. 2006. PRIMER v6. User manual/Tutorial. PRIMER-E, Plymouth.

Collado-Fabbri, S., Vaulot, D. & Ulloa, O. 2011. Structure and seasonal dynamics of the eukaryotic picophytoplankton community in a wind-driven coastal upwelling ecosystem. Limnology and Oceanography, 56: 2334-2346. doi: 10.4319/lo.2011.56.6.2334

Cullen, J.J. 2015. Subsurface chlorophyll maximum layers: enduring enigma or mystery solved? Annual Review of Marine Science, 7: 207-239. doi: 10.1146/annurev-marine-010213-135111

DuRand, M.D., Olson, R.J. & Chisholm, S.W. 2001. Phytoplankton population dynamic at the Bermuda Atlantic time-series station in the Sargasso Sea. Deep-Sea Research - Part II, 48: 1983-2003. doi: 10.1016/S0967-0645(00)00166-1

Duret, M.T., Pachiadaki, M.G., Stewart, F.J., Sarode, N., Christaki, U., Monchy, S., et al. 2015. Size-fractionated diversity of eukaryotic microbial communities in the eastern tropical North Pacific oxygen minimum zone. FEMS Microbiology Ecology, 91: 1-12. doi: 10.1093/femsec/fiv037

Edler, L. & Elbrächter, M. 2010. The Utermöhl method for quantitative phytoplankton analysis. In: Karlson, B., Cusack, C. & Bresnan, E. (Eds.). Microscopic and molecular methods for quantitative phytoplankton analysis. UNESCO & IOC, Paris, pp. 13-20.

Escobar-Morales, S. & Hernández-Becerril, D.U. 2015. Free-living marine planktonic unarmoured dinoflagellates from the Gulf of Mexico and the Mexican Pacific. Botanica Marina, 58: 9-22. doi: 10.1515/bot-2014-0049

Esqueda-Lara, K. & Hernández-Becerril, D.U. 2010. Dinoflagelados microplanctónicos marinos del Pacífico central de México (Isla Isabel, Nayarit y costas de Jalisco y Colima). Universidad Nacional Autónoma de México, Ciudad de México.

Esqueda-Lara, K., Hernández-Becerril, D.U. & Robles-Jarero, E.G. 2005. Annual cycle of microphytoplankton from coasts of the tropical Mexican Pacific. Cahiers de Biologie Marine, 46: 335-345.

Franz, J., Krahmann, G., Lavik, G., Grasse, P., Dittmar, T. & Riebesell, U. 2012. Dynamics and stoichiometry of nutrients and phytoplankton in waters influenced by the oxygen minimum zone in the eastern tropical Pacific. Deep-Sea Research - Part I, 62: 20-31. doi: 10.1016/j.dsr.2011.12.004

Gallegos, A., Rodríguez, R., Márquez, E., Lecuanda, R. & Zavala-Hidalgo, J. 2006. Una climatología de la temperatura de la superficie del mar de las aguas adyacentes a las costas de Jalisco, Colima y Michoacán, México, 1996-2003. In: Jiménez-Quiroz, M.C. & Espino- Barr, E. (Eds.). Los recursos pesqueros y acuícolas de Jalisco, Colima y Michoacán. SAGARPA-INAPESCA, Ciudad de México, pp. 17-28.

Gérikas-Ribeiro, C., Lopes dos Santos, A., Marie, D., Pellizari, V.H., Brandini, F.P. & Vaulot, D. 2016. Pico and nanoplankton abundance and carbon stocks along the Brazilian bight. Peer Journal, 4: e2587.

Gibb, S.W., Barlow, R.G., Cummings, D.G., Rees, N.W., Trees, C.C., Holligan, P., et al. 2000. Surface phytoplankton pigment distributions in the Atlantic Ocean, an assessment of basin scale variability between 50ºN and 50ºS. Progress in Oceanography, 45: 339-368. doi: 10.1016/S0079-6611(00)00007-0

Goericke, R., Olson, R.J. & Shalapyonok, A. 2000. A novel niche for *Prochlorococcus* sp. in low-light suboxic environments in the Arabian Sea and the Eastern Tropical North Pacific. Deep-Sea Research -

Part I, 47: 1183-1205. doi: 10.1016/S0967-0637(99)00108-9

González-Ferreiro, D. & Bosque-Sendra, J. 2008. Generación de un mapa de vientos en un SIG. Boletín de la Asociación de Geógrafos Españoles, 47: 51-77.

González-García, C., Forja, J., González-Cabrera, M.C., Jiménez, M.P. & Lubián, L.M. 2018. Annual variations of total and fractionated chlorophyll and phytoplankton groups in the Gulf of Cadiz. Science of the Total Environment, 613-614: 1551-1565.

Grasshoff, K., Ehrhardt, M. & Kremling, K. 1983. Methods of seawater analysis. Verlag Chemie, Berlin.

Hernández-Becerril, D.U. 1996. A morphological study of *Chaetoceros* species (Bacillariophyta) from the plankton of the Pacific Ocean of Mexico. Bulletin of the Museum of Natural History (Botany), 26: 1-73. doi: 10.1080/0269249X.2002.9705552

Hernández-Becerril, D.U. 1998. Species of the planktonic diatom *Pseudo-nitzschia* of the Pacific coasts of Mexico. Hydrobiologia, 379: 77-84. doi: 10.1023/A:1003471828302

Hernández-Becerril, D.U. & Bravo-Sierra, E. 2001. Planktonic silicoflagellates (Dictyochophyceae) from the Mexican Pacific. Botanica Marina, 44: 417-423. doi: 10.1515/BOT.2001.050

Hernández-Becerril, D.U. & Bravo-Sierra, E. 2004. New records on planktonic dinoflagellates (Dinophyceae) from the Mexican Pacific Ocean. Botanica Marina, 47: 417-423. doi: 10.1515/BOT.2004.051

Hernández-Becerril, D.U. & Vega-Juárez, G. 2022. Morphology of the marine, planktonic, thecate dinoflagellate *Gonyaulax areolata* (Dinophyceae), a species causing red tides in the tropical Mexican Pacific. Phycologia, 61: 595-605. doi: 10.1080/00318884.2022.2108659

Hernández-Becerril, D.U., Barón-Campis, S.A. & Escobar-Morales, S. 2012a. A new record of *Azadinium spinosum* (Dinoflagellata) from the tropical Mexican Pacific. Revista de Biología Marina y Oceanografía, 47: 553-557. doi: 10.4067/S0718-19572012000300016

Hernández-Becerril, D.U., Esqueda-Lara, K. & Torres-Martínez, R. 2016. Cocolitofóridos. Taxonomía de especies presentes en mares de México (Pacífico occidental, Golfo de California, Pacífico central y Golfo de México). MAPorrúa, Ciudad de México.

Hernández-Becerril, D.U., Barón-Campis, S.A., Salazar-Paredes, J. & Alonso-Rodríguez, R. 2013. Species of the planktonic diatom genus *Skeletonema* (Bacillariophyta) from the Mexican Pacific Ocean. Cryptogamie, Algologie, 34: 77-87. doi: 10.7872/crya.v34.iss2.2013.77

Hernández-Becerril, D.U., Herrera-Hernández, P., Pérez-Mendoza, L.A. & Ceballos-Corona, J.G.A. 2010. Marine planktonic diatoms of the order Rhizosoleniales (Bacillariophyta) from the tropical Mexican Pacific. Vie et Milieu, 60: 95-107.

Hernández-Becerril, D.U., Aquino-Cruz, A., Salas-de-León, D.A. Signoret-Poillon, M. & Monreal-Gómez, M.A. 2012b. Studies on picophytoplankton in the southern Gulf of Mexico, pigment analysis and potential importance of the picoeukaryote Prasinophyte *Micromonas pusilla*. Marine Biology Research, 8: 331-340. doi: 10.1080/17451000.2011.638639

Hernández-Becerril, D.U., Ceballos-Corona, J.G.A., Esqueda-Lara, K., Tovar-Salazar, M.A. & León-Álvarez, D. 2008. Marine planktonic dinoflagellates of the order Dinophysiales (Dinophyta) from coasts of the tropical Mexican Pacific, including two new species of the genus *Amphisolenia*. Journal of the Marine Biological Association of the UK, 88: 1-15. doi: 10.1017/S0025315408000143

Hernández-Becerril, D.U., Lau, W.L.S., Hii, K.S., Leaw, C.P., Varona-Cordero, F. & Lim, P.T. 2018. Abundance and distribution of the potentially toxic thecate dinoflagellate *Alexandrium tamiyavanichii* (Dinophyceae) in the central Mexican Pacific, using the quantitative PCR method. Frontiers in Marine Science, 5: 366. doi: 10.3389/fmars.2018.00366

Hernández-Becerril, D.U., Alonso-Rodríguez, R., Álvarez-Góngora, C., Barón-Campis, S.A., Ceballos-Corona, J.G.A., Herrera-Silveira, J., et al. 2007. Toxic and harmful marine phytoplankton and microalgae (HABs) in Mexican coasts. Journal of Environmental Science and Health Part A, 42: 1349-1363. doi: 10.1080/10934520701480219

Jing, H., Rocke, E., Kong, L., Xia, X., Liu, H. & Landry, M.R. 2015. Protist communities in a marine oxygen minimum zone off Costa Rica by 454 pyrosequencing. Biogeosciences Discussions, 12: 13483-13509.

Kirkham, A.R., Lepère, C., Jardillier, L.E., Not, F., Bouman, H., Mead, A. & Scanlan, D.J. 2013. A global perspective on marine photosynthetic picoeukaryote community structure. ISME Journal, 7: 922-936. doi: 10.1038/ismej.2012.166

Kirkwood, D.S. 1994. Sanplus segmented flow analyzer and its applications. Seawater analysis. Skalar, Bogotá.

Larios-Muñiz, M., González-Silvera, A., Castro, R., Santamaría-del-Ángel, E., Collins, C.A. & López-Calderón, J. 2022. Variability of hydrographic factors,

biomass and structure of the phytoplankton community at the entrance to the Gulf of California (spring 2013). Continental Shelf Research, 235: 104665.

Latasa, M., Scharek, R., Le Gall, F. & Guillou, L. 2004. Pigment suites and taxonomic groups in Prasinophyceae. Journal of Phycology, 40: 1149-1155.

Lavin, P., González, B., Santibáñez, J.F., Scanlan, D.J. & Ulloa, O. 2010 Novel lineages of *Prochlorococcus* thrive within the oxygen minimum zone of the eastern tropical South Pacific. Environmental Microbiology Reports, 2: 728-738. doi: 10.1111/j.1758-2229.2010.00167.x

Lee, S. & Fuhrman, J.A. 1987. Relationships between biovolume and biomass of naturally derived marine bacterioplankton. Applied and Environmental Microbiology, 53: 1298-1303. doi: 10.1128/aem.53.6.1298-1303.1987

Linacre, L.P., Landry, M.R., Lara-Lara, J.R., Hernández-Ayón, J. & Bazán-Guzmán, C. 2010. Picoplankton dynamics during contrasting seasonal oceanographic conditions at a coastal upwelling station off northern Baja California, Mexico. Journal of Plankton Research, 32: 539-557. doi: 10.1093/plankt/fbp148

López-Sandoval, D.C., Lara-Lara, J.R., Lavín, M.F., Álvarez-Borrego, S. & Gaxiola-Castro, G. 2009. Productividad primaria en el Pacífico oriental tropical adyacente a Cabo Corrientes, México. Ciencias Marinas, 35: 169-182.

Marañón, E. 2015. Cell size as a key determinant of phytoplankton metabolism and community structure. Annual Review of Marine Science, 7: 241-264. doi: 10.1146/annurev-marine-010814-015955

Marie, D., Partensky, F., Vaulot, D. & Brussard, C. 1999. Enumeration of phytoplankton, bacteria, and viruses in marine samples. In: Robingson, J.P., Darzynkiewicz, Z., Dean, P.N., Orfao, A., Rabinovitch, P., Stewart, C.C., et al. (Eds.). Current protocols in cytometry. John Wiley & Sons, New Jersey.

Márquez-Artavia, A., Sánchez-Velasco, L., Barton, E.D., Paulmier, A., Santamaría-del-Ángel, E. & Beier, E. 2019. A suboxic chlorophyll-*a* maximum persists within the Pacific oxygen minimum zone off Mexico. Deep-Sea Research - Part II, 169-170: 104686. doi: 10.1016/j.dsr2.2019.104686

Maske, H., Escobar, E., Sánchez, L., Olmeda-Jauregui, C.O., Chapa-Balcorta, C., Sosa-Avalos, R., et al. 2019. Zona del mínimo de oxígeno en el Pacífico mexicano. In: Paz-Pellat, F., Hernández-Ayón, J.M., Sosa-Ávalos, R. & Velázquez-Rodríguez, A.S. (Eds.). Estado del ciclo del carbono: Agenda azul y verde. Secretaría de Pesca, Ciudad de México, pp. 86-102.

Miranda-Álvarez, C., González-Silvera, A., Santamaría-del-Angel, E., López-Calderón, J., Godínez, V.M., Sánchez-Velasco, L., et al. 2020. Phytoplankton pigments and community structure in the northeastern tropical Pacific using HPLC-CHEMTAX analysis. Journal of Oceanography, 76: 91-108. doi: 10.1007/s10872-019-00528-3

Moreno, D.V., Marrero, J.P., Morales, J., Llerandi-García, C., Villagarcía, U., Rueda, M.J., et al. 2012. Phytoplankton functional community structure in Argentinian continental shelf determined by HPLC pigment signatures. Estuarine, Coastal and Shelf Science, 100: 72-81. doi: 10.1016/j.ecss.2012.01.007

Not, F., Latasa, M., Marie, D., Cariou, T., Vaulot, D. & Simon, N. 2004. A single species, *Micromonas pusilla* (Prasinophyceae), dominates the eukaryotic picoplankton in the western English Channel. Applied and Environmental Microbiology, 70: 4064-4072. doi: 10.1128/aem.70.7.4064-4072.2004

Ortiz-Lira, H. & Jiménez-Quiroz, M.C. 2006. Registro de eventos de marea roja en Manzanillo, Colima (1986-2004). In: Jiménez-Quiroz, M.C. & Espino-Barr, E. (Eds.). Los recursos pesqueros y acuícolas de Jalisco, Colima y Michoacán. Secretaría de Pesca, Ciudad de México, pp. 324-334.

Pajares, S., Varona-Cordero, F. & Hernández-Becerril, D.U. 2020. Spatial distribution patterns of bacterioplankton in the oxygen minimum zone of the tropical Mexican Pacific. Microbial Ecology, 80: 519-536. doi: 10.1007/s00248-020-01508-7

Parris, D.J., Ganesh, G., Edgcomb, V.P., DeLong, E.F. & Stewart, F.J. 2014. Microbial eukaryote diversity in the marine oxygen minimum zone off northern Chile. Frontiers in Microbiology, 5: 1-11. doi: 10.3389/fmicb.2014.00543

Paulmier, A. & Ruiz-Pino, D. 2009. Oxygen minimum zones (OMZs) in the modern ocean. Progress in Oceanography, 80: 113-128. doi: 10.1016/j.pocean.2008.08.001

Pelayo-Martínez, G., Olivos-Ortiz, A., Franco-Gordo, C., Quijano-Scheggia, S., Gaviño-Rodriguez, J., Kono-Martínez, T., et al. 2017. Physical, chemical and zooplankton biomass variability (inshore-offshore) of Mexican central Pacific during El Niño-La Niña 2010. Latin American Journal of Aquatic Research, 45: 67-78. doi: 10.3856/vol45-issue1-fulltext-7

Ras, J., Claustre, H. & Uitz, J. 2008. Spatial variability of phytoplankton pigment distributions in the subtropical south Pacific Ocean, comparison between *in situ* and predicted data. Biogeosciences, 5: 353-369.

Rocap, G., Distel, D., Waterbury, J.B. & Chisholm, S.W. 2002. Resolution of *Prochlorococcus* and *Synecho-*

coccus ecotypes by using 16S-23S ribosomal DNA internal transcribed spacer sequences. Applied and Environmental Microbiology, 68: 1180-1191. doi: 10.1128/aem.68.3.1180

Rodríguez, F., Chauton, M., Johnsen, G., Andresen, K., Olsen, L.M. & Zapata, M. 2006. Photoacclimation in phytoplankton, implications for biomass estimates, pigment functionality and chemotaxonomy. Marine Biology, 148: 963-971. doi: 10.1007/s00227-005-0138-7

Santana-Vega, Z., Hernández-Becerril, D.U., Morales-Blake, A.R., Varona-Cordero, F. & Merino-Ibarra, M. 2018. Prokaryotic picoplankton distribution within the oxygen minimum zone of the central Mexican Pacific across environmental gradients. Brazilian Journal of Oceanography, 66: 157-171. doi: 10.1590/s1679-87592018004806602

Sunagawa, S., Coelho, L.P., Chaffron, S., Kultima, J.R., Labadie, K., Salazar, G., et al. 2015. Ocean plankton. Structure and function of the global ocean microbiome. Science, 348: 1261359. doi: 10.1126/science.1261359

Suzuki, K., Hinuma, A., Saito, H., Kiyosawa, H., Liu, H., Saino, T., et al. 2005. Responses of phytoplankton and heterotrophic bacteria in the northwest subarctic Pacific to *in situ* iron fertilization as estimated by HPLC pigment analysis and flow cytometry. Progress in Oceanography, 64: 167-187. doi: 10.1016/j.pocean.2005.02.007

Tamm, M., Laas, P., Freiberg, R., Nõges, T. & Nõges, P. 2018. Parallel assessment of marine autotrophic picoplankton using flow cytometry and chemotaxonomy. Science of the Total Environment, 625: 185-193. doi: 10.1016/j.scitotenv.2017.12.234

Tragin, M.L., dos Santos, A., Christen, R. & Vaulot, D. 2016. Diversity and ecology of green microalgae in marine systems: an overview based on 18S rRNA gene sequences. Perspectives in Phycology, 3: 141-154. doi: 10.1127/pip/2016/0059

Uitz, J., Claustre, H., Morel, A. & Hooker, S. 2006. Vertical distribution of phytoplankton communities in open ocean, an assessment based on surface chlorophyll. Journal of Geophysical Research, 111: C08005. doi: 10.1029/2005JC003207

Ulloa, O., Canfield, D.E., DeLong, E.F., Letelier, R.M. & Stewart, F.J. 2012. Microbial oceanography of anoxic oxygen minimum zones. Proceedings of the National Academy of Sciences, 109: 15996-16003. doi: 10.1073/pnas.1205009109

Vega-Juárez, G. 2014. Caracterización de las proliferaciones algales ocurridas en el Pacífico central mexicano del 10 al 22 de abril del 2012. M.Sc. Thesis, Universidad Nacional Autónoma de México, Ciudad de México.

Veldhuis, M.J.W. & Kraay, G.W. 1990. Vertical distribution and pigment composition of a picoplanktonic prochlorophyte in the subtropical North Atlantic, a combined study of HPLC- analysis of pigments and flow cytometry. Marine Ecology Progress Series, 68: 121-127. doi: 10.3354/meps068121

Vidussi, F., Claustre, H., Bustillos-Guzmán, J., Cailliau, C. & Marty, J.C. 1996. Rapid HPLC method for determination of phytoplankton chemotaxonomic pigments, separation of chlorophyll *a* from divinyl-chlorophyll-*a* and zeaxanthin from lutein. Journal of Plankton Research, 18: 2377-2382. doi: 10.1093/plankt/18.12.2377

Vieira-Araujo, M.L., Borges-Mendes, C.R., Tavano, V.M., Eiras-García, C.A. & Baringer, M.O. 2017. Contrasting patterns of phytoplankton pigments and chemotaxonomic groups along 30°S in the subtropical south Atlantic Ocean. Deep-Sea Research - Part I, 120: 112-121. doi: 10.1016/j.dsr.2016.12.004

Wang, F., Xie, Y., Wu, W., Sun, P., Wang, L. & Huang, B. 2019. Picoeukaryotic diversity and activity in the northwestern Pacific Ocean based on rDNA and rRNA high-throughput sequencing. Frontiers in Microbiology, 9: 1-13. doi: 10.3389/fmicb.2018.03259

Ward, B.A., Dutkiewicz, S. & Follows, M.J. 2014. Modelling spatial and temporal patterns in size-structured marine plankton communities, top-down and bottom-up controls. Journal of Plankton Research, 36: 31-47. doi: 10.1093/plankt/fbt097

Worden, A.Z. 2006. Picoeukaryote diversity in coastal waters of the Pacific Ocean. Aquatic Microbial Ecology, 43: 165-175. doi: 10.3354/ame043165

Worden, A.Z. & Not, F. 2008. Ecology and diversity of picoeukaryotes. In: Kirchman, D.L. (Ed.). Microbial ecology of the oceans. John Wiley & Sons, New Jersey, pp. 159-204.

Wrigth, S.W. & Mantoura, E.F.C. 1997. Guidelines for collection and pigment analysis on field samples. In: Jeffrey, S.W., Mantoura, R.F.C. & Wright, S.W. (Eds.). Phytoplankton pigments in oceanography. Guidelines to modern methods. UNESCO, Paris.

Wright, J.J., Konwar, K.M. & Hallam, S.J. 2012. Microbial ecology of expanding oxygen minimum zones. Nature Reviews Microbiology, 10: 381-394. doi: 10.1038/nrmicro2778

Yung, C.C.M., Redondo, E.R., Sánchez, F., Yau, S. & Piganeau, G. 2022. Diversity and evolution of

Mamiellophyceae: Early-diverging phytoplanktonic green algae containing many cosmopolitan species. Journal of Marine Science and Engineering, 10: 240. doi: 10.3390/jmse10020240

Received: August 7, 2023; Accepted: March 5, 2024

Table S1. Variables and samples measured and collected in the five zones of the study area, and stations and depths considered. CTD profiles included measurements of temperature, salinity, dissolved oxygen, and fluorescence (chlorophyll-*a*). Pigments were samples for HPLC analysis. Flow cytometry was sampled for picophytoplankton analysis, and phytoplankton was sampled for microscopic phytoplankton analysis.

Zone	Station (Depth, m)	CTD profiles	Pigments	Flow cytometry	Phytoplankton
Cabo Corrientes	5 (1 m)	X	X	X	
	5 (5 m)		X	X	
	5 (20 m)		X	X	X
	5 (40 m)		X	X	X
	5 (83 m)		X	X	X
	7 (1 m)		X	X	X
	7 (5 m)		X	X	
	7 (31 m)		X	X	X
	7 (50 m)				X
	7 (73 m)		X	X	
	9 (1 m)		X	X	
	9 (5 m)				X
	9 (23 m)				X
	9 (40 m)				X
Bahía Manzanillo	23 (1 m)	X	X	X	
	23 (18 m)		X	X	
	23 (40 m)		X	X	
	21 (1 m)		X	X	
	21 (5 m)		X	X	
	21 (23 m)		X	X	
	21 (40 m)		X	X	
	21 (61 m)		X	X	
	20a (1 m)		X	X	
	20a (5 m)		X	X	
	20a (20 m)		X	X	
	20a (40 m)		X	X	
Maruata	31 (1 m)	X	X	X	
	31 (5 m)		X	X	
	31 (21 m)		X	X	
	31 (40 m)		X	X	
	31 (75 m)		X	X	
	29 (1 m)		X	X	
	29 (32 m)		X	X	
	29 (40 m)		X	X	
	29 (85 m)		X	X	
	28a (1 m)		X	X	
	28a (5 m)		X	X	
	28a (20 m)		X	X	
	28a (40 m)		X	X	
	28a (77 m)		X	X	

Continuation

Zone	Station (Depth, m)	CTD profiles	Pigments	Flow cytometry	Phytoplankton
Lázaro Cárdenas	34 (1 m)	X	X	X	
	34 (15 m)		X	X	
	34 (18 m)		X	X	
	34 (40 m)		X	X	
	34 (75 m)		X	X	
	37 (1 m)		X	X	
	38a (1 m)		X	X	
	38a (15 m)		X	X	
	38a (20 m)		X	X	
	38a (42 m)		X	X	
	38a (85 m)		X	X	
Acapulco	42 (1 m)	X	X	X	
	42 (10 m)		X	X	
	42 (40 m)		X	X	
	45 (1 m)		X	X	
	45 (15 m)		X	X	
	45 (20 m)		X	X	
	45 (38 m)		X	X	
	46a (1 m)		X	X	
	46a (15 m)		X	X	
	46a (20 m)		X	X	
	46a (46 m)		X	X	
	46a (77 m)		X	X	